Table 2. HLA-A, -B, and -C alleles in patients with cADRs

HLA allele	Japanese population allele frequency[a] (%)	Group A (mild cADR) Allele frequency	Group A (mild cADR) Relative risk	Group B (severe cADR) Allele frequency	Group B (severe cADR) Relative risk
A*0201	10.9	0/20	0.00	2/10	2.03
A*0206	10.4	1/20	0.46	1/10	0.96
A*0207	3.4	2/20	3.11	0/10	0.00
A*1101	8.1	2/20	1.26	0/10	0.00
A*2402	35.6	10/20	1.80	5/10	1.80
A*2601	9.8	0/20	0.00	1/10	1.03
A*2603	2.1	2/20	5.37	0/10	0.00
A*3101	7.7	2/20	1.33	1/10	1.33
A*3303	7.9	1/20	0.61	0/10	0.00
B*1302	0.1	0/20	0.00	0/10	0.00
B*1501	7.2	2/20	1.45	0/10	0.00
B*1518	0.9	0/20	0.00	1/10	13.58
B*3501	8.6	2/20	1.19	1/10	1.19
B*4001	5.1	1/20	0.99	0/10	0.00
B*4002	8.2	1/20	0.60	1/10	1.26
B*4006	5.3	1/20	0.95	0/10	0.00
B*4403	6.9	0/20	0.00	0/10	0.00
B*4601	3.8	3/20	4.40	2/10	6.24
B*4801	2.7	1/20	1.94	1/10	4.10
B*5101	7.9	3/20	2.05	0/10	0.00
B*5201	13.7	3/20	1.10	0/10	0.00
B*5401	6.5	2/20	1.60	1/10	1.60
B*5502	3.2	1/20	1.57	1/10	3.31
B*5901	1.7	0/20	0.00	2/10	15.16
B*6701	1.0	0/20	0.00	0/10	0.00
C*0102	17.0	5/18	1.87	4/10	3.23
C*0103	r	1/18		0/10	
C*0303	7.8	1/18	0.71	2/10	3.00
C*0304	11.3	3/18	1.60	1/10	0.89
C*0401	6.5	1/18	0.92	0/10	0.00
C*0602	1.7	0/18	0.00	0/10	0.00
C*0702	11.3	1/18	0.47	0/10	0.00
C*0704	0.9	0/18	0.00	1/10	12.89
C*0801	10.9	2/18	1.00	1/10	0.89
C*1202	10.4	2/18	1.09	0/10	0.00
C*1402	5.7	2/18	1.96	0/10	0.00
C*1502	1.7	0/18	0.00	1/10	6.39

HLA, human leucocyte antigen.

[a]HLA*A & B, Tanaka et al. Clinical Transplants 1996; 139–144; HLA*C, Tokunaga et al. Immunogenetics 1997, 46: 199–205.

HLA-B

Ten patients in group A and five patients in group B were analyzed. In group A, relative risk was highest for HLA-B*4601 allele (4.40), and zero in HLA-B*4403 allele among alleles with relatively high frequencies in the Japanese population. In group B, relative risks were high for HLA-B*1518 (13.58) and HLA-B*5901 alleles (15.16), and zero in HLA-B*1501, HLA-B*4403, HLA-B*5101, and HLA-B*5201 alleles among alleles with relatively high frequencies in the Japanese population.

HLA-C

Nine patients in group A and five patients in group B were analyzed. In group A, relative risks that can be calculated were lower than 2.0. Although C*0103 was detected in one patient only in group A, the relative risk could not be calculated because of rare frequency in the Japanese population. In group B, relative risks were high for HLA-C*0704 allele (12.89) and HLA-C*1502 allele (6.39), and zero for HLA-C*0702 and HLA-C*1202 alleles among alleles with relatively high frequencies in the Japanese population.

HLA A-B-C haplotype

Relative risks of the A-B-C haplotype were calculated depending on data of the Japanese population. The haplotype HLA-A*2402-B*5901-C*0102 and the haplotype HLA-A*0201-B*1518-C*0704 were found in two and one patient of group B, respectively. The relative risks of the former haplotype and the latter haplotype for severe cADRs are 16.09 and 28.94, respectively.

Discussion

We have experienced many patients manifesting cADR at various levels of severity induced by AEDs. A total of 21,655 patients with epilepsy visited our epilepsy center up until 2006, and 166 patients (0.767%) experienced cADRs. Among them, 139 patients experienced cADRs causally related to AEDs, with 118 patients (0.545%) having mild cADRs (group A) and 21 patients (0.097%) having severe cADRs (group B) (Takahashi, 2007). Various attempts have been made to identify individuals at high risk of developing severe cADRs with intolerable sequelae. In the Han Chinese (Chung et al., 2004; Hung et al., 2005) and the Thai population (Locharernkul et al., 2008), a strong association between HLA-B*1502 and CBZ-induced SJS has been found. Our previous studies found that HLA-B*1502 is a rare allele in Japanese, and that no Japanese patients with CBZ-induced SJS have HLA-B*1502 (Kaniwa et al., 2008; Kashiwagi et al., 2008). Following these studies, we found that HLA-B*1518, HLA-B*5901, and HLA-C*0704 alleles showed higher relative risks above 10.0 in the extended group of patients with severe cADRs (group B). Although HLA-B*1518 and HLA-C*0704 alleles were found in only one patient, HLA-B*5901 was found in two patients in group B (B-2 and B-5). The haplotype HLA-A*2402-B*5901-C*0102 has a prevalence of 1.530% in the Japanese population. The relative risk of this haplotype for severe cADRs is 16.09. These data may suggest that HLA-B*5901 is a candidate marker of CBZ-induced SJS. The relative risk of HLA-B*5901 for CBZ-induced SJS (15.16) is higher than that for pemphigus vulgaris (DR4, relative risk = 14), acute anterior uveitis

(B27, 10), and systemic lupus erythematosus (DR3, 6), but lower than that for ankylosing spondylitis (B27, 87) and Goodpasture syndrome (DR2, 16) (Marsh et al., 2000). HLA-B*5901 has been reported to be weakly associated with SJS/TEN with ocular complications in a Japanese study (Ueta et al., 2008), although this study included patients with SJS/TEN independent of offending drugs. Further studies will reveal the significance of HLA-B*5901 in SJS/TEN induced by CBZ.

HLA-B*5801 is reported to be strongly associated with severe cADRs caused by allopurinol in Han Chinese (Hung et al., 2005). HLA-B*5701 is reported to be strongly associated with a hypersensitivity reaction caused by abacavir in U.S. white and black patients (Saag et al., 2008). Because the amino acid sequence of HLA-B*5901 shares 93.9% homology with that of HLA-B*5701, and 95.0% homology with that of HLA-B*5801, the homology of amino acid residues among these HLA subtypes seems to be high. Therefore, HLA-B*5901 may be causally related to severe cADRs induced by CBZ. Further investigations with a larger number of patients with CBZ-induced SJS are required to confirm the involvement of HLA-B*5901 in CBZ-induced SJS in the Japanese population. We expect that this report would encourage HLA examinations in Japanese patients, leading to the development of prevention methods for CBZ-induced SJS.

Our data suggest that possible HLA class I markers for mild cADRs induced by CBZ are completely different from those for SJS. In the Thai population also, HLA-B*1502 had a strong association only with CBZ-induced SJS, but not with CBZ-induced maculopapular eruptions (Locharernkul et al., 2008). Therefore, differentiation between severe cADRs and mild cADRs in each patient is very important to confirm the true markers for CBZ-induced SJS. In patients with severe cADRs, frequencies of HLA-A*1101, HLA-A*3303, HLA-B*1501, HLA-B*4403, HLA-B*5101, HLA-B*5201, HLA-C*0702, and HLA-C*1202 alleles are relatively lower than in the Japanese population. Whether these HLA class I markers are inhibitory for SJS may be answered in the future through precise immunologic studies.

Acknowledgments

This study was funded in part by Health and Labour Sciences Research Grants for Research on Human Genome Tailor made (H18-002), and on Psychiatry and Neurological Diseases and Mental Health (H20-021); Research Grants (19A-6) for Nervous and Mental Disorders from the Ministry of Health, Labor and Welfare; and grants-in-aid for Scientific Research I No. 16590859, 17591133, and 19591234.

Disclosure: We have read the Journal's position on issues involved in ethical publication and affirm that this report is consistent with those guidelines. None of the authors has any conflicts of interest to disclose.

References

Chung WH, Hung HS, Hong HS, Hsih MS, Yang LC, Ho HC, Wu JY, Chen YT. (2004) Medical genetics: a marker for Stevens–Johnson syndrome. *Nature* 428:486.

Hung SI, Chung WH, Liou LB, Chu CC, Lin M, Huang HP, Lin YL, Lan JL, Yang LC, Hong HS, Chen MJ, Lai PC, Wu MS, Chu CY, Wang KH, Chen CH, Fann CS, Wu JY, Chen YT. (2005) HLA-B*5801 allele as a genetic marker for severe cutaneous adverse reactions caused by allopurinol. *Proc Natl Acad Sci U.S.A.* 15:4134–4139.

Hung SI, Chung WH, Jee SH, Chen WC, Chang YT, Lee WR, Hu SL, Wu MT, Chen GS, Wong TW, Hsiao PF, Shih HY, Fang WH, Wei CY, Lou YH, Lin JJ, Chen YT. (2006) Genetic susceptibility to carbamazepine-induced cutaneous adverse drug reactions. *Pharmacogenet Genomics* 16:297–306.

Kaniwa N, Saito Y, Aihara M, Matsunaga K, Tohkin M, Kurose K, Sawada J, Furuya H, Takahashi Y, Muramatsu M, Kinoshita S, Abe M, Ikeda H, Kashiwagi M, Song Y, Ueta M, Sotozono C, Ikezawa Z, Hasegawa R; JSAR research group. (2008) HLA-B locus in Japanese patients with anti-epileptics and allopurinol-related Stevens–Johnson syndrome and toxic epidermal necrolysis. *Pharmacogenomics* 9:1617–1622.

Kashiwagi M, Aihara M, Takahashi Y, Yamazaki E, Yamane Y, Yixuan S, Muramatsu M, Ikezawa Z. (2008) HLA genotypes in carbamazepine-induced severe cutaneous adverse drug response in Japanese patients. *J Dermatol* 10:683–685.

Locharernkul C, Loplumlert J, Limotai C, Korkij W, Desudchi T, Tongkobpetch S, Kangwanshiratada O, Hirankarn N, Suphapeetiporn K, Shotelersuk V. (2008) Carbamazepine and phenytoin induced Stevens–Johnson syndrome is associated with HLA-B*1502 allele in Thai population. *Epilepsia* 49:2087–2091.

Marsh SGE, Parham P, Barber LD. (2000) *The HLA facts book.* Academic Press, London.

Roujeau JC, Kelly JP, Naldi L, Rzany B, Stern RS, Anderson T, Auquier A, Bastuji-Garin S, Correia O, Locati F, Mockenhaupt M, Paoletti C, Shapiro S, Shear N, Schöpf E, Kaufman DW. (1995) Medication use and the risk of Stevens–Johnson syndrome or toxic syndrome or toxic epidermal necrolysis. *N Engl J Med* 333:1600–1607.

Saag M, Balu R, Phillips E, Brachman P, Martorell C, Burman W, Stancil B, Mosteller M, Brothers C, Wannamaker P, Hughes A, Sutherland-Phillips D, Mallal S, Shaefer M. (2008) Study of Hypersensitivity to Abacavir and Pharmacogenetic Evaluation Study Team. High sensitivity of human leukocyte antigen-b*5701 as a marker for immunologically confirmed abacavir hypersensitivity in white and black patients. *Clin Infect Dis* 1:1111–1118.

Takahashi Y. (2007) Study of HLA in patients of severe cutaneous reaction by AEDs and controls. In Kaniwa N (Eds) *Report of investigation about diagnosis, treatment and genetic markers in severe cutaneous reaction (H18-002).* Ministry of Health, Labor and Welfare, Tokyo, pp. 33–35.

Ueta M, Tokunaga K, Sotozono C, Inatomi T, Yabe T, Matsushita M, Mitsuishi Y, Kinoshita S. (2008) HLA class I and II gene polymorphisms in Stevens–Johnson syndrome with ocular complications in Japanese. *Mol Vis* 14:550–555.

Journal of association of diseases/symptoms

Atypical Miller Fisher syndrome associated with glutamate receptor antibodies

Taku Hatano,[1] Yoshiaki Shimada,[1] Ayako Kono,[1] Shin-ichiro Kubo,[2] Kazumasa Yokoyama,[1] Asako Yoritaka,[1] Toshiki Nakahara,[1] Yukitoshi Takahashi,[3] Nobutaka Hattori[1]

[1]Department of Neurology, Juntendo University, School of Medicine, Hongo, Bunkyo-ku, Tokyo, Japan;
[2]Department of Neurology, Juntendo Tokyo Koto Geriatric Medical Center, Shinsuna, Koto-ku, Tokyo, Japan;
[3]National Epilepsy Center, Shizuoka MIND, Urushiyama, Shizuoka, Japan

Correspondence to Taku Hatano, thatano@juntendo.ac.jp

Summary

The present study reports a young woman with acute ataxia, areflexia and ophthalmoplegia, accompanied by psychosis and involuntary movements (IVMs) from disease onset. Anti-GQ1b and anti-GT1a antibodies were detected allowing for a diagnosis of Miller Fisher syndrome (MFS). However, psychosis and IVMs are atypical MFS symptoms and often mimic symptoms of anti-N-methyl-D-aspartate receptor (NMDAR) encephalitis. Interestingly, the autoantibodies against full-length glutamate receptor-ε2 (GluRε2) and glutamate NR2B- and NR2A-containing heteromers (NR1/NR2) of NMDAR were also detected in the patient serum and cerebrospinal fluid. It was concluded that psychosis and IVMs in this patient were associated with autoantibodies against various GluRs.

BACKGROUND

Miller Fisher syndrome (MFS) is an autoimmune disorder accompanied by acute progressive ophthalmoplegia, ataxia and areflexia. Bickerstaff's brainstem encephalitis (BBE) is a related syndrome in which central nervous system (CNS) features, such as altered consciousness and/or long tract signs, accompany classic triad.[1 2] Ganglioside GQ1b antibodies are often associated with both conditions, resulting in the proposal that MFS and BBE might be closely related and form a continuous disease.[3] Among the clinical features of both MFS and BBE, psychosis and involuntary movements (IVMs) are atypical.[4] The present case reports a young woman who presented with acute cerebellar ataxia, areflexia and ophthalmoplegia, which was accompanied by psychosis and IVMs from disease onset. Serum serological tests revealed high anti-GQ1b and anti-GT1a antibody titres. In addition, serum and cerebrospinal fluid (CSF) tests also detected high antibody titres against NR2B- and NR2A-containing heteromers of N-methyl-D-aspartate receptor (NMDAR) and antiglutamate receptor-ε2 (GluRε2).

CASE PRESENTATION

A 23-year-old woman presented initially with double vision and a mild, unsteady gait and was admitted to our hospital in May 2008. One week earlier, the patient experienced a respiratory infection. On the first day of illness, the patient suffered from transient double vision and dizziness. The following day, the patient was restless, agitated and cried incomprehensively. Symptoms rapidly exacerbated following hospital admission (day 2); the patient was alert, but exhibited emotional incontinence and personality changes. Extraocular movement was inhibited in all directions and conjugate eye movements were impaired with coarse nystagmus. Facial muscles were weak and the patient presented with slurred speech and dysphagia. Marked cerebellar ataxia was present in the finger-nose and heel-knee test. Muscle tone decreased and deep tendon reflexes of the upper and lower extremities were absent. The Babinski response was bilaterally negative and limb muscle strength and sensory examination were normal.

On day 3, the patient became somnolent and screamed irritably like a child. Both pupils were dilated and light reflexes were diminished. The patient developed orolingual IVMs, such as lip-licking, chewing, dyskinesia and myoclonic movements. Psychosis and IVMs mimicked features of patients with ovarian teratoma-associated encephalitis[5] (video 1). Hypersalivation was also exhibited, but hypoventilation or seizures did not develop.

INVESTIGATIONS

Routine blood analyses, including thyroid functions, were normal. Serum antibodies specific to HIV, syphilis, neurotrophic viruses, *Mycoplasma pneumoniae*, thyroid disease and autoimmune disease (antinuclear, anti-SS-A/SS-B antibodies, MPO-ANCA, PR3-ANCA and anticardiolipin antibodies) were insignificant. CSF analysis revealed a white blood cell count of 14/ml, 24 mg protein/dl and negative PCR results for herpes simplex virus genome. EEGs showed a slightly irregular basic pattern without epileptic discharge. Nerve conduction velocities and compound muscle action potentials were normal, with a significant decrease in F-wave amplitude of median and tibial nerves. Brainstem auditory-evoked potentials and cranial MRI, with or without gadolinium enhancement revealed no abnormalities. Chest, abdominal and pelvic CT were normal. ^{123}I-iodoamphetamine single photon emission CT (^{123}I-IMP SPECT), which was performed on day 13, revealed hypoperfusion in the brainstem, cerebellum, thalamus and frontotemporal cortices. Follow-up ^{123}I-IMP

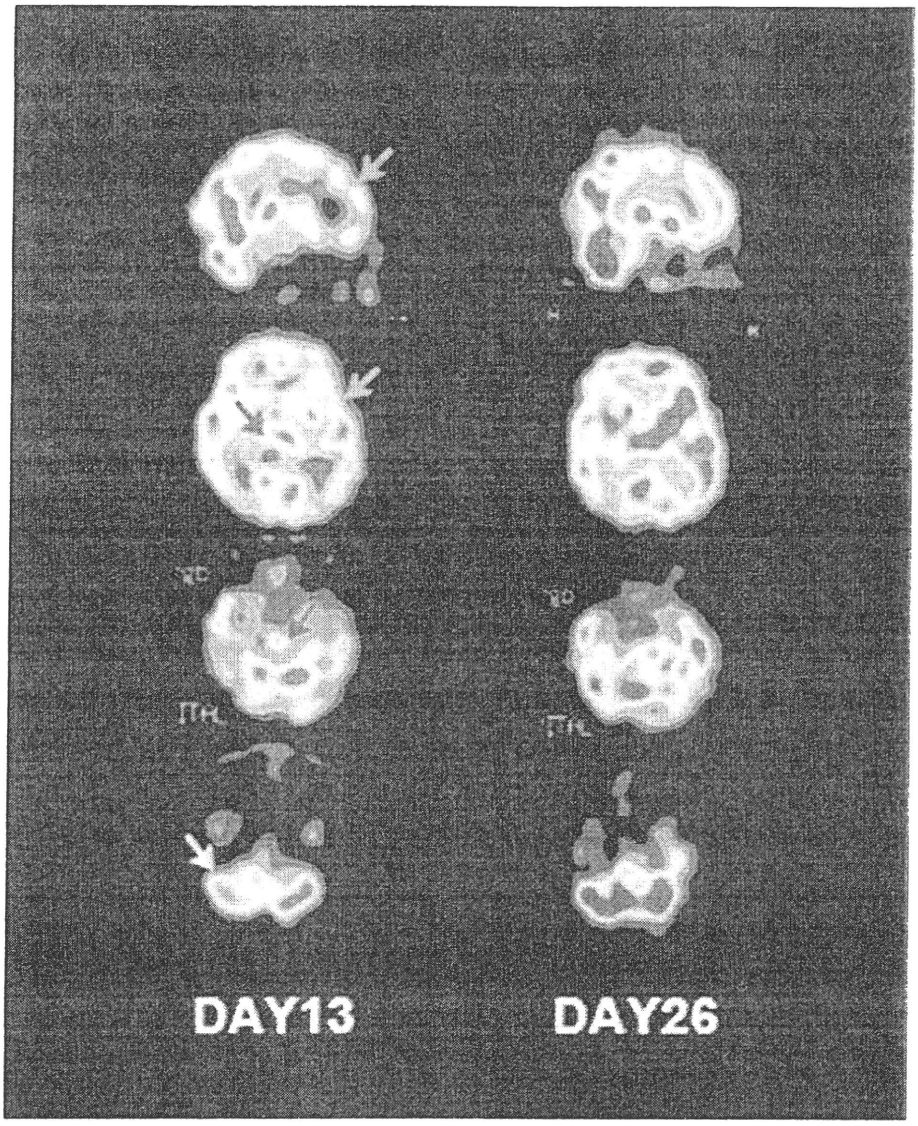

Figure 1 ^{123}I-iodoamphetamine single photon emission CT (^{123}I-IMP SPECT) imaging of the patient. On day 13, ^{123}I-IMP SPECT reveals decreased rCBF in the frontotemporal cortex (green arrows), thalamus (blue arrow), brainstem (red arrow) and cerebellum (yellow arrow) (A). Follow-up ^{123}I-IMP SPECT on day 26 shows improvement in the damaged lesion (B).

SPECT on day 26 demonstrated perfusion recovery in these lesions (figure 1).

Video 1 The patient exhibits ophthalmoplegia, coarse nystagmus, sluggish papillary light reflex and involuntary movements around the eyebrows and mouth. The patient also screams irritably like a child.10.1136/bcr.08.2010.3228v1

DIFFERENTIAL DIAGNOSIS AND TREATMENT

These findings suggested the diagnosis of atypical MFS-related disorder accompanied by psychosis and IVMs. Therefore, the patient was administered intravenous immunoglobulin (Ig) (20 g/day for 5 days), followed by intravenous methylprednisolone (1 g/day for 3 days). On day 10, the patient developed rough and coarse IVMs, which affected the left arm, despite improved psychiatric behaviour. Subsequently, the patient received intravenous methylprednisolone, accompanied by steroid tapering.

ELISA revealed that serum samples from day 3 contained high IgG antibody titres to GQ1b and GT1a. Furthermore, antibodies to full-length GluRε2 (anti-GluRε2 antibodies) and glutamate NR2B- and NR2A-containing heteromers of NMDAR (anti-NR1/NR2 antibodies) were examined as described previously.[6] Anti-NR1/NR2 antibodies, as well as anti-GluRε2 IgG and IgM antibodies, were expressed in serum and CSF on day 3. On day 16, serum anti-GluRε2 IgM antibody levels were reduced, but IgG antibodies remained present.

OUTCOME AND FOLLOW-UP

Although the symptoms lasted for 2 weeks, improvement was considerable with intact neurological symptoms within 6 weeks of disease onset. After 1 year, the patient exhibited no neurological complications and pelvic MRI was normal.

DISCUSSION

Clinical findings fulfilled diagnostic criteria for MFS.[2] However, the patient also presented with atypical clinical features, such as psychosis and IVMs. In addition, anti-NR1/NR2 antibodies and anti-GluRε2 antibodies were present. ^{123}I-IMP SPECT examinations demonstrated that patient symptoms were due to impaired cortex, thalamus, cerebellum and brainstem. Interestingly, Wada *et al*, also described two BBE patients with delirium[4]; both patients fulfilled the diagnostic criteria for BBE, including positive serum titres for anti-GQ1b and -GT1a antibodies, as well as childish behaviours and emotional incontinence. The patients also exhibited rigidity and IVMs, such as tremors and hypertonia in the masseter muscles, which mimicked tetanus. SPECT analysis revealed hypoperfusion of the frontal lobe, brainstem and basal ganglia, which was similar to results from the present study. Although atypical psychosis and IVMs in these patients were possibly due to autoantibodies against various GluRs, including anti-GluRε2 antibodies and anti-NR1/NR2 antibodies, the association between these antibodies was not discussed in the paper.

Dalumau *et al* reported that limbic encephalitis is a result of anti-NR1/NR2 antibodies associated with ovarian teratoma, which has been termed anti-NMDAR encephalitis.[5] Clinical characteristics of patients with anti-NMDAR encephalitis include psychosis, seizures, IVMs, autonomic instability and central hypoventilation. Anti-GluRε2 antibody is described as an association between non-herpetic limbic encephalitis[6–8] and epilepsia partialis continua-related Rasmussen encephalitis.[9] Several studies have shown that anti-GluRε2 and anti-NR1/NR2 antibodies are detectable in patients with non-herpetic limbic encephalitis.[7 8] Kamei *et al* reported the clinical features of acute juvenile female non-herpetic encephalitis (AJFNHE) in Japan based on a nationwide questionnaire,[8] with a detection rate of autoantibodies against several GluRs of 67%. Clinical AJFNHE phenotypes closely mimic anti-NMDAR encephalitis, including psychosis and IVMs, and anti-NR1/NR2 antibodies have been detected in several patients with AJFNHE.[8] The GluRε2 subunit NR2A functions as an NMDAR component. Huerta *et al* reported that NR2 autoantibodies induce emotional abnormality in mice.[10] These studies suggested that autoantibodies against some GluR subunits could result in psychosis and IVMs in our patient.

The mechanism by which ganglioside (anti-GQ1b and anti-GT1a) and GluR antibodies were co-expressed in the patient, thereby triggering clinical features, remains unknown. There is a high prevalence of prodromal viral-like symptoms in anti-NMDAR encephalitis and AJFNHE.[5 8] Moreover, Gable *et al* reported that 4/10 patients with anti-NMDAR encephalitis exhibit serological evidence of acute Mycoplasma infection.[11] Although the number of cases in this study was very small, with a high amount of false IgM positivity results, Mycoplasma infection should be considered, as Mycoplasma could contain epitopes mimicking both GQ1b ganglioside and GluRs. The patient did not express Mycoplasma-specific IgM antibodies; however, a prodromal respiratory infection was diagnosed. Therefore, it is possible that a microorganism could trigger antibody production against these antigens, as detected in the patient.

- Patients with MFS and related disorders rarely present with atypical psychosis and IVMs such as delirium, oral dyskinesia, tremor or myoclonus.
- CNS involvement, such as psychosis and IVMs in patients with atypical MFS-related disorders could be associated with various anti-GluR antibodies.

Acknowledgements The authors thank Dr Susumu Kusunoki (Department of Neurology, Kinki University) and Dr Keiko Tanaka (Department of Neurology, Kanazawa Medical University) for measuring antiganglioside antibodies and anti-NMDA receptor antibody, respectively.

Competing interests None.

Patient consent Obtained.

REFERENCES

1. **Odaka M,** Yuki N, Yamada M, *et al*. Bickerstaff's brainstem encephalitis: clinical features of 62 cases and a subgroup associated with Guillain-Barré syndrome. *Brain* 2003;**126**(Pt 10):2279–90.
2. **Overell JR,** Willison HJ. Recent developments in Miller Fisher syndrome and related disorders. *Curr Opin Neurol* 2005;**18**:562–6.
3. **Odaka M,** Yuki N, Hirata K. Anti-GQ1b IgG antibody syndrome: clinical and immunological range. *J Neurol Neurosurg Psychiatr* 2001;**70**:50–5.
4. **Wada Y,** Yanagihara C, Nishimura Y, *et al*. Delirium in two patients with Bickerstaff's brainstem encephalitis. *J Neurol Sci* 2008;**269**:184–6.
5. **Dalmau J,** Gleichman AJ, Hughes EG, *et al*. Anti-NMDA-receptor encephalitis: case series and analysis of the effects of antibodies. *Lancet Neurol* 2008;**7**:1091–8.
6. **Tachibana N,** Shirakawa T, Ishii K, *et al*. Expression of various glutamate receptors including N-methyl-D-asparate receptor (NMDAR) in an ovarian teratoma removed from a young woman with anti-NMDAR encephalitis. *Inter Med* 2010;**49**:2167–73.
7. **Takahashi Y.** Epitope of autoantibodies to N-methyl-D-aspartate receptor heteromers in paraneoplastic limbic encephalitis. *Ann Neurol* 2008;**64**: 110–11; author reply 111–12.
8. **Kamei S,** Kuzuhara S, Ishihara M, *et al*. Nationwide survey of acute juvenile female non-herpetic encephalitis in Japan: relationship to anti-N-methyl-D-asparate receptor encephalitis. *Inter Med* 2009;**48**:673–9.
9. **Takahashi Y,** Mori H, Mishina M, *et al*. Autoantibodies and cell-mediated autoimmunity to NMDA-type GluRε2 in patients with Rasmussen's encephalitis and chronic progressive epilepsia partialis continua. *Epilepsia* 2005;**46**:152–8.
10. **Huerta PT,** Kowal C, DeGiorgio LA, *et al*. Immunity and behavior: antibodies alter emotion. *Proc Natl Acad Sci USA* 2006;**103**:678–83.
11. **Gable MS,** Gable S, Radner A, *et al*. Anti-NMDA receptor encephalitis: report of ten cases and comparison with viral encephalitis. *Eur J Clin Microbiol Infect Dis* 2009;**28**:1421–9.

This pdf has been created automatically from the final edited text and images.

Copyright 2011 BMJ Publishing Group. All rights reserved. For permission to reuse any of this content visit
http://group.bmj.com/group/rights-licensing/permissions.
BMJ Case Report Fellows may re-use this article for personal use and teaching without any further permission.

Please cite this article as follows (you will need to access the article online to obtain the date of publication).

Hatano T, Shimada Y, Kono A, Shin-ichiro K, Yokoyama K, Yoritaka A, Nakahara T, Takahashi Y, Hattori N. Atypical Miller Fisher syndrome associated with glutamate receptor antibodies. *BMJ Case Reports* 2011;10.1136/bcr.08.2010.3228, date of publication

Become a Fellow of BMJ Case Reports today and you can:
- Submit as many cases as you like
- Enjoy fast sympathetic peer review and rapid publication of accepted articles
- Access all the published articles
- Re-use any of the published material for personal use and teaching without further permission

For information on Institutional Fellowships contact consortiasales@bmjgroup.com

Visit casereports.bmj.com for more articles like this and to become a Fellow

Journal of the Neurological Sciences 296 (2010) 59–63

Contents lists available at ScienceDirect

Journal of the Neurological Sciences

journal homepage: www.elsevier.com/locate/jns

A Japanese ALS6 family with mutation R521C in the *FUS/TLS* gene: A clinical, pathological and genetic report☆

Yukiko Yamamoto-Watanabe [a], Mitsunori Watanabe [a,b,*], Koichi Okamoto [b], Yukio Fujita [b], Mandy Jackson [c], Masaki Ikeda [b], Yoichi Nakazato [d], Yoshio Ikeda [e], Etsuro Matsubara [a], Takeshi Kawarabayashi [a], Mikio Shoji [a]

[a] *Department of Neurology, Hirosaki University Graduate School of Medicine, Hirosaki, Aomori 036-8562, Japan*
[b] *Department of Neurology, Gunma University Graduate School of Medicine, Maebashi, Gunma 371-8511, Japan*
[c] *Centre of Integrative Physiology, University of Edinburgh, Summerhall, Edinburgh, UK*
[d] *Department of Human Pathology, Gunma University Graduate School of Medicine, Maebashi, Gunma 371-8511, Japan*
[e] *Department of Neurology, Graduate School of Medicine, Dentistry and Pharmaceutical Sciences, Okayama, Okayama 700-8558, Japan*

ARTICLE INFO

Article history:
Received 10 February 2010
Received in revised form 28 May 2010
Accepted 7 June 2010

Keywords:
ALS6
Familial amyotrophic lateral sclerosis
FUS/TLS
Phenotype
Proximal muscle atrophy
Sternocleidomastoideus

ABSTRACT

Here we report a Japanese family with amyotrophic lateral sclerosis (ALS) characterized by very rapid progression, high penetrance and an autosomal dominant mode of inheritance. The phenotype includes atrophy of sternocleidomastoideus muscles, bulbar involvement, weakness of neck muscles and proximal muscle atrophy. These clinical symptoms are reminiscent of myopathy. All patients examined had similar clinical symptoms, age at onset and disease duration. The proband was found to have mutation R521C in the *FUS/TLS* gene, and was diagnosed as having ALS6. Autopsy material was available from the mother of the proband and FUS-immunoreactive neuronal and glial cytoplasmic inclusions were observed in the anterior horn of the spinal cord. While atrophy and weakness of the sternocleidomastoideus muscle is not emphasized in previous reports, this symptom may be a clinical hallmark of ALS6.

© 2010 Elsevier B.V. All rights reserved.

1. Introduction

Amyotrophic lateral sclerosis (ALS) is a fatal neurodegenerative disease, for which no effective therapy is available. It is characterized by generalized skeletal muscle weakness and atrophy due to degeneration of upper and lower motor neurons [1,2]. Only a small proportion of ALS cases (5–10%) have a family history of the disease, and this subset of patients is classified as familial ALS (FALS). To date, a number of genetic loci and disease causing mutations have been identified in FALS patients [3]. Mutations in Cu/Zn superoxide dismutase (*SOD1*) give rise to ALS1 [4,5], whereas mutations in *FUS/TLS* [6,7], *VAPB* [8], *ANG* [9] and *TDP-43* [10,11] give rise to ALS6, ALS8, ALS9 and ALS10, respectively. So far gene mutations have not been identified for ALS3 [12] or ALS7 [13] which show typical ALS phenotypes [14]. Other genes are responsible for forms of familial ALS that show distinctive clinical features from those of typical ALS such as juvenile onset, slow progression, spastic paraparesis, or dementia [15–19]. Here we report a Japanese family with autosomal dominant familial ALS whose clinical features are almost identical between individuals. Of note, proximal muscles are more severely affected than distal ones, and atrophy of the sternocleidomastoideus muscles and weakness of the neck muscles is obvious, reminiscent of myopathy. However they conformed to the El Escorial criteria of ALS and the proband was found to have mutation R521C in the *FUS/TLS* gene. Furthermore neuronal and glial cytoplasmic FUS-positive inclusions were observed in the anterior horn of the spinal cord. The present report clearly shows ALS6 cases occur in Japan, and the clinical and pathological features are atrophy of sternocleidomastoideus muscle, bulbar signs, weakness of the neck muscles, proximal muscle atrophy, rapid progression and FUS-immunoreactive neuronal and glial cytoplasmic inclusions in the anterior horn of the spinal cord.

2. Case report

Clinical features along with biochemical and physiological measurements are summarized for three members of a Japanese pedigree in Table 1.

Abbreviations: SOD1, Cu/Zn superoxide dismutase; ALS, amyotrophic lateral sclerosis.

☆ Disclosure: The authors report no conflict of interest.

* Corresponding author. Department of Neurology, Hirosaki University Graduate School of Medicine, Hirosaki, Aomori 036-8562, Japan. Tel.: +81 172 39 5142; fax: +81 172 39 5143.
E-mail address: miwata36@cc.hirosaki-u.ac.jp (M. Watanabe).

0022-510X/$ – see front matter © 2010 Elsevier B.V. All rights reserved.
doi:10.1016/j.jns.2010.06.008

Table 1
Clinical data on the present ALS6 family.

	Patient 1 (II-3)	Patient 2 (II-1)	Patient 3 (I-4)
Sex	Female	Male	Female
Age at onset (yr)	38	32	29
Survival period (mo)	26/110[a]	7	15
Intellectual disturbance	–	–	–
Site of onset	Bulbar	Lower limbs	Lower limbs
Mechanical ventilation	+	–	–
Creatine kinase	170/127[b] (normal 20–110 IU/l)	66 (normal 0–170 mU/ml)	NE
Total cholesterol (mg/dl)	254/211[b]	154	NE
High-density lipoprotein cholesterol (mg/dl) 40		NE	NE
Serum hexosamidase A activity	Normal	NE	NE
Cerebrospinal fluid findings			
Total cell count (/μl)	<1	<1	0
Protein (mg/dl)	22	48	Not quantified
Sugar (mg/dl)	64	58	71
NCS (motor and sensory)	Normal	Normal	NE
Needle EMG (all limbs)	Neurogenic	Neurogenic	Neurogenic

–, absent; +, present; NE, not examined; NCS, nerve conduction study; EMG, electromyogram.
[a] The numbers show interval between the onset of symptoms and beginning of ventilator support, and total disease duration, respectively.
[b] The values of these items were examined twice.

2.1. Patient 1

A 38-year-old Japanese female (proband, Subject II-3 in Fig. 1) had difficulty in excreting sputa. She soon developed difficulties eating and exhibited fatigue when chewing. At almost the same time, she developed dysarthria, gait disturbance and had difficulty in raising her left arm. She began to repeatedly fall down and at the age of 39 she could no longer stand up from the sitting position without assistance. Thereafter difficulty with excreting sputa, gait disturbance and weakness in chewing worsened and she was admitted to our hospital. On physical examination, she was alert, found to be slightly obese and had hypertension. Examination of the optic fundi showed findings of hypertension and atherosclerosis, but no optic atrophy or retinal degeneration. Her mental status was normal, and her verbal, performance, and full-scale scores of Wechsler Adult Intelligence Scale were 93, 107 and 99, respectively. Although her ocular movements were normal, she had atrophy and weakness in the masseter muscles. She also had a nasal voice, dysphagia, severe atrophy and weakness in the bilateral sternocleidomastoideus muscles, and atrophy and fasciculation in the tongue. She had proximally dominant muscle atrophy and weakness in all limbs, and muscle tonus was generally decreased. She could not flex her neck in the supine position due to very severe weakness in the neck muscles. Scores of manual muscle testing (MMT) of the flexor and extensor muscles of the neck were 2/5 and 4/5, respectively. She had to walk her hands up her legs in order to stand from a kneeling position (Gowers sign (+)). Snout, jaw, and palmomental reflexes were positive. The deep tendon reflexes were slightly increased in the upper limbs and slightly decreased in the lower limbs. The plantar responses were bilaterally extensor. She had very mild hypalgesia and hypesthesia in her left thigh and lower legs, whereas she had neither rectal and bladder disturbance nor cerebellar signs.

The serum levels of creatine kinase and total cholesterol were slightly elevated as shown in Table 1. Brain computed tomogram and magnetic resonance image were normal. Studies on somatosensory evoked potentials showed normal findings although some theta but not epileptiform activity was present in the electroencephalogram. Muscle biopsy was performed in the left quadriceps and the specimens displayed small angulated fibers and fiber type grouping. Thereafter her clinical symptoms progressed very rapidly, and she required ventilator support approximately 26 months after the onset of symptoms. By the age of 45, she showed very severe atrophy and weakness in general skeletal muscles, but her ocular movements were preserved and communication was possible with eye movement. Subsequently she had repeated pneumonia, and died of respiratory failure at the age of 47. An autopsy could not be performed.

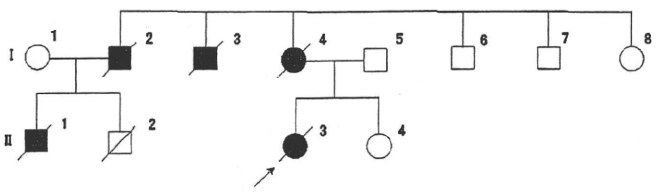

Fig. 1. Pedigree tree of a Japanese family with ALS6.

2.2. Genetic analysis

Blood samples with informed consent were obtained from this patient, and 73 normal controls, and genomic DNA was isolated by a standard phenol/chloroform method. The five exons of SOD1, the six exons of VAPB, and the single coding exon of angiogenin, including exon–intron boundaries, were amplified by polymerase chain reaction (PCR) and sequenced as previously described [8,9,20,21]. No mutation was identified in any of these genes. Exons 1, 9, 10, 11, 12 and 13 of MAPT (TAU) were also screened, but no mutation was detected. According to a published method [7], the 15 exons of the *FUS/TLS* gene were amplified by PCR, and directly sequenced. For reproducible sequencing results, exon 15 was sequenced using an internal reverse primer, 5-cttgggtgatcaggaattgg-3. As a result, a disease-causing mutation, c.1561 C>T (R521C) was detected in exon 15 in the *FUS/TLS* gene (Fig. 2). To rule out the possibility of sequencing errors, the PCR products from exon 15 were subcloned into the TA vector (Invitrogen, Carlsbad, CA) and sequenced. The missense mutation was also confirmed by AlwI restriction digest of PCR product (344 bp) (New England Biolabs, Tokyo, Japan). Wild-type allele when digested produces a 218- and 126-bp fragment, whereas the mutant allele is not cut. This PCR-restriction fragment length polymorphism (RFLP) analysis confirmed patient 1 was heterozygous for the wild-type and mutant allele with both cut and uncut products being observed (Fig. 3). Of 72 normal Japanese controls subjected to RFLP, all showed homozygosity for the wild-type allele. Two synonymous polymorphisms, c.147 C>A in exon 3 and c.291 C>T in exon 4 were also detected in this patient.

2.3. Patient 2

Patient 2 (Subject II-1 in Fig. 1), a 32-year-old male, showed gait disturbance, and gradually developed dysarthria. Approximately

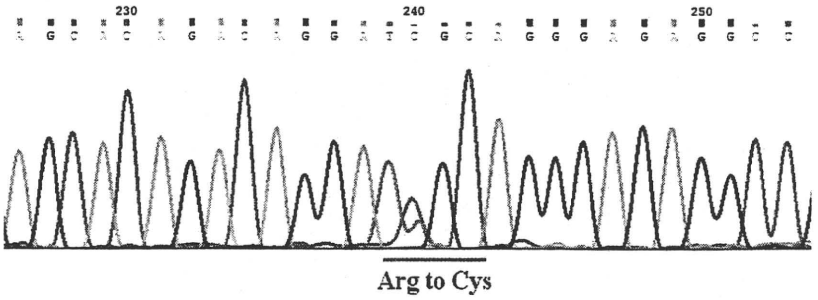

Fig. 2. Sequence of exon 15 of *FUS/TLS* from patient 1. DNA mutation and resulting amino acid change (arginine to cysteine) is shown by the red line.

three months after onset of disease he began to have difficulty in flexing his neck in the supine position and often fell down. On examination, his mental status was normal. He had severe atrophy in the bilateral sternocleidomastoideus muscles, fasciculation in the facial muscles, and atrophy and fasciculation in the tongue. He had dysarthria and his voice was slightly nasal. He also had severe weakness of the neck flex muscle (score of MMT: 2/5) and proximally dominant muscle weakness of the upper limbs. Muscle tonus was normal in the upper limbs, but increased in the lower limbs. Bilateral biceps, triceps, patellar and Achilles tendon reflexes were increased, and plantar responses were bilaterally flexor. His symptoms deteriorated very rapidly, and he died from respiratory failure approximately seven months after the onset of symptoms. An autopsy could not be performed.

2.4. Patient 3

Patient 3 (Subject I-4 in Fig 1), a 29-year-old female, started to notice that she walked dragging her left leg, and frequently stumbled. Approximately five months later she developed muscle weakness in her right leg and both arms. One month later her gait disturbance worsened, and she noticed hypesthesia in the bilateral lower legs. She was still able to use her hands without difficulty, but she could not raise her arms and stand up from the supine position without support. She also had difficulties taking deep breaths. One month later her mobility was reduced to crawling. Approximately one year after onset of symptoms she began to have difficulty in excreting sputa and developed dyspnea. Only then was she admitted to our hospital. On physical examination, she was alert and had no dementia. She had no obvious hypertension and the findings of the optic fundi were normal. She displayed severe muscle atrophy and weakness in all limbs, and scapular winging. She had hypesthesia in the bilateral lower legs. She continued to suffer from severe pneumonia, and died of respiratory failure almost three months after admission. The total disease duration was approximately 15 months. An autopsy was carried out and we examined paraffin-embedded sections of the cervical, thoracic and lumbar cord. Anterior horn cells were severely lost, and extensive astrocytic gliosis was observed. No Bunina bodies were found but some basophilic inclusions were seen in the surviving anterior horn cells (Fig. 4A). Klüver–Barrera staining showed mild diffuse myelin pallor in the anterolateral columns but not in the posterior columns. Finally immunohistochemistry revealed FUS-positive cytoplasmic inclusions in some surviving neurons within the anterior horns and intermediate substance (Fig. 4B–D). FUS-positive cytoplasmic inclusions were also seen in some glial cells in the anterior horn and lateral funiculus and judging from morphology thought to be oligodendrocytes (Fig. 4E). Cytoplasmic inclusions also stained positive for ubiquitin (Fig. 4F) and some p62-positive structures could be discerned (data not shown). However, no pTDP-43-positive inclusions, such as skein-like or round inclusions, were observed in the cytoplasm of anterior horn cells. Antibodies used were a rabbit polyconal antibody against FUS (A300-302A, 1:250, Bethyl, Montgomery, TX), a rabbit polyclonal anti-ubiquitin antibody (1:2,000, Dako, Denmark), a guinea pig monoclonal antibody against the amino-terminus of p62 (1:2000, Progen Biotechnik, Heidelberg, Germany) and a rabbit polyclonal anti-phosphorylated TDP-43 (pTDP-43) antibody[22].

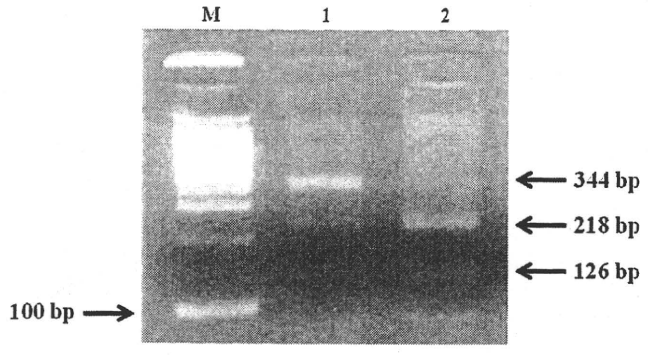

Fig. 3. AlwI restriction digest of genomic PCR products of exon 15 of the *FUS/TLS* gene from patient 1 (lane 1) and normal control (lane 2). Control lane shows two digested products (218 bp and 126 bp), whereas an undigested band (344 bp) remains in patient lane. 100-bp ladder shown on left (lane M).

3. Discussion

The main clinical features of this family are an age of onset in the late twenties to late thirties, atrophy and weakness of the sternocleidomastoideus muscles, bulbar signs including nasal voice, weakness of the neck muscles, a greater involvement of proximal skeletal muscles than distal ones, and a very rapid progression of disease. Dementia has never been observed. On examination, patient 3 had diffuse atrophy and weakness in all limbs, but presumably at the beginning of disease had proximally dominant muscle weakness given her clinical course and the occurrence of scapular winging. Based on the distribution of affected muscles this may have led to a misdiagnosis of myopathy such as polymyositis or limb-girdle muscular dystrophy. However patients 1 and 2 conformed to the diagnostic criteria outlined by the El Escorial classification for ALS [1], and pathological findings of patient 3 were compatible with ALS. Stewart et al. have reported a family with a SOD1 mutation (G72C) that clinically mimicks myopathy, whereas most cases with a SOD1 mutation have distal onset in one limb [23]. The family reported here with clinical symptoms similar to myopathy has no mutation in the SOD1 gene but has a mutation in the *FUS/TLS* gene (R521C). Immunohistochemical analysis confirmed the occurrence of FUS-positive neuronal and cytoplasmic inclusions in the anterior horn of the spinal cord.

Ticozzi et al. previously reported ALS cases with the R521C mutation display more proximal than distal muscle involvement, similar to our findings. Conversely a patient with another mutation, G156E has more distal muscle weakness [24]. A study by Corrado et al. [25] reports that the initial clinical symptoms of patients with the

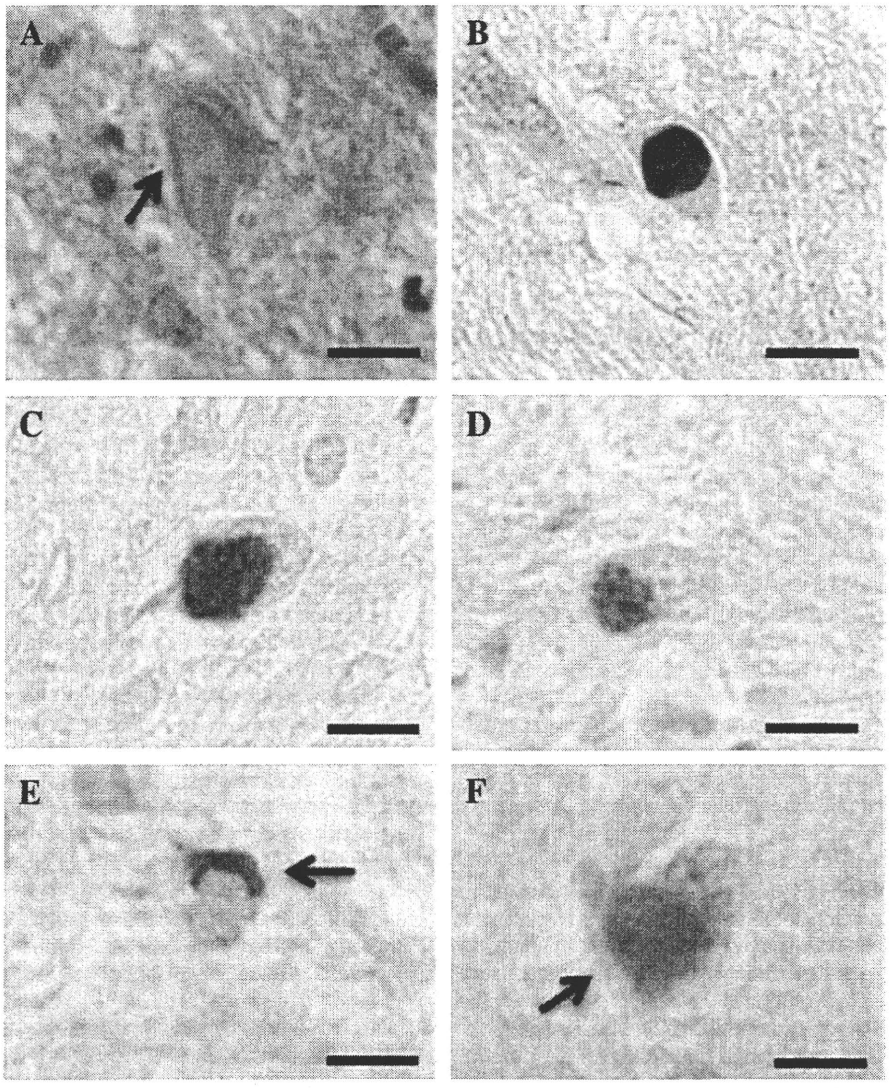

Fig. 4. Immunohistochemistry of spinal cord sections from patient 3. (A) H & E staining shows anterior horn cell with basophilic inclusion (arrow). (B–D) FUS-positive cytoplasmic inclusions present in surviving motor neurons. (E) Glial cell with a FUS-positive cytoplasmic inclusion which appears to be an oligodendrocyte. (F) Ubiquitin-positive cytoplasmic inclusion in anterior horn cell (arrow). Scale bar 20 μm (A–D, F); 5 μm (E).

R521C mutation are weakness of the neck flexor/extensor muscles and proximal upper limb weakness. The R521C mutation was also found in a Canadian sporadic ALS patient, but there is no clinical history [26]. Taken together the findings suggest that initial symptoms associated with the R521C mutation are weakness of the neck and proximal muscles but age at onset, topography of affected muscles and time course are more variable (Table 1)[24,25]. Regarding ALS1, clinical variation is seen among patients with the same SOD1 genotype and within members of the same family [14], except for A4V which correlates with shorter survival 27]. However, although there is some variability in ALS6 cases, the clinical symptoms of patients with the R521C mutation appear to be more homogenous. Whether the topography of affected muscles is specific to the R521C mutation or common to other ALS6 patients is not clear but it should be pointed out that a patient with mutation R521H has distally dominant lower limb weakness [28]. Although an association between atrophy of sternocleidomastoideus muscles and ALS has never previously been highlighted, this symptom may be related to weakness of the neck muscles and could be a hallmark of ALS6. In order to clarify this, further investigation with a larger number of cases is required. Furthermore the proband and her mother had hypesthesia in their legs, and this symptom may be associated with the observed mild diffuse myelin pallor seen in the anterolateral columns of patient 3.

Recent work suggests a new biochemical category of neurodegenerative disease in terms of aberrant accumulation of FUS (FUS proteinopathy) [29,30]. Many groups are proposing a similar role of FUS and TDP-43 in neuronal death since both are ubiquitously expressed DNA/RNA-binding proteins involved in multiple nuclear functions [6,7,29,30]. Future studies are needed to examine the exact role of mutant FUS in neurodegenerative disorders such as ALS6.

Acknowledgements

We are extremely grateful to all patients studied for their cooperation and support. We also thank Ms. I. Shirahama, Drs. J. Kaneko, S. Hirai and T. Yanagisawa for their kind support. This study was supported by Grants-in Aid for Primary Amyloidosis Research Committee (M Yamada), from the Ministry of Health, Labor and Welfare of Japan, by Grant-in Aid for Scientific Research (B) (19390233), by Grant-in Aid for Scientific Research (C) (22590921), by The Mochida Memorial Foundation for Medical and Pharmaceutical Research, and by the grant provided by Sapporo Biocluster "Bio-S", the Knowledge Cluster Initiative of the MEXT. This work was also supported by grants from the Ministry of Health, Labour and Welfare of Japan and from the Ministry of Education, Culture, Sports, Science and Technology of Japan.

References

[1] Mitsumoto H, Chad DA, Pioro EP. Amyotrophic lateral sclerosis. Philadelphia: F.A. Davis; 1998.
[2] Cleveland DW, Rothstein JD. From Charcot to Lou Gehrig: deciphering selective motor neuron death in ALS. Nat Rev Neurosci 2001;2:806–19.
[3] Valdmanis PN, Daoud H, Dion PA, Rouleau GA. Recent advances in the genetics of amyotrophic lateral sclerosis. Curr Neurol Neurosci Rep 2009;9:198–205.
[4] Deng HX, Hentati A, Tainer JA, Iqbal Z, Cayabyab A, Hung WY, et al. Amyotrophic lateral sclerosis and structural defects in Cu, Zn superoxide dismutase. Science 1993;261:1047–51.
[5] Rosen DR, Siddique T, Patterson D, Figlewicz DA, Sapp P, Hentati A, et al. Mutations in Cu/Zn superoxide dismutase gene are associated with familial amyotrophic lateral sclerosis. Nature 1993;362:59–62.
[6] Kwiatkowski Jr TJ, Bosco DA, Leclerc AL, Tamrazian E, Vanderburg CR, Russ C, et al. Mutations in the FUS/TLS gene on chromosome 16 cause familial amyotrophic lateral sclerosis. Science 2009;323:1205–8.
[7] Vance C, Rogelj B, Hortobagyi T, De Vos KJ, Nishimura AL, Sreedharan J, et al. Mutations in FUS, an RNA processing protein, cause familial amyotrophic lateral sclerosis type 6. Science 2009;323:1208–11.
[8] Nishimura AL, Mitne-Neto M, Silva HC, Richieri-Costa A, Middleton S, Cascio D, et al. A mutation in the vesicle-trafficking protein VAPB causes late-onset spinal muscular atrophy and amyotrophic lateral sclerosis. Am J Hum Genet 2004;75:822–31.
[9] Greenway MJ, Andersen PM, Russ C, Ennis S, Cashman S, Donaghy C, et al. ANG mutations segregate with familial and 'sporadic' amyotrophic lateral sclerosis. Nat Genet 2006;38:411–3.
[10] Sreedharan J, Blair IP, Tripathi VB, Hu X, Vance C, Rogelj B, et al. TDP-43 mutations in familial and sporadic amyotrophic lateral sclerosis. Science 2008;319:1668–72.
[11] Kabashi E, Valdmanis PN, Dion P, Spiegelman D, McConkey BJ, Vande Velde C, et al. TARDBP mutations in individuals with sporadic and familial amyotrophic lateral sclerosis. Nat Genet 2008;40:572–4.
[12] Hand CK, Khoris J, Salachas F, Gros-Louis F, Lopes AA, Mayeux-Portas V, et al. A novel locus for familial amyotrophic lateral sclerosis, on chromosome 18q. Am J Hum Genet 2002;70:251–6.
[13] Sapp PC, Hosler BA, McKenna-Yasek D, Chin W, Gann A, Genise H, et al. Identification of two novel loci for dominantly inherited familial amyotrophic lateral sclerosis. Am J Hum Genet 2003;73:397–403.
[14] Kunst CB. Complex genetics of amyotrophic lateral sclerosis. Am J Hum Genet 2004;75:933–47.
[15] Hadano S, Hand CK, Osuga H, Yanagisawa Y, Otomo A, Devon RS, et al. A gene encoding a putative GTPase regulator is mutated in familial amyotrophic lateral sclerosis 2. Nat Genet 2001;29:166–73.
[16] Yang Y, Hentati A, Deng HX, Dabbagh O, Sasaki T, Hirano M, et al. The gene encoding alsin, a protein with three guanine-nucleotide exchange factor domains, is mutated in a form of recessive amyotrophic lateral sclerosis. Nat Genet 2001;29:160–5.
[17] Chen YZ, Bennett CL, Huynh HM, Blair IP, Puls I, Irobi J, et al. DNA/RNA helicase gene mutations in a form of juvenile amyotrophic lateral sclerosis (ALS4). Am J Hum Genet 2004;74:1128–35.
[18] Moreira MC, Klur S, Watanabe M, Nemeth AH, Le Ber I, Moniz JC, et al. Senataxin, the ortholog of a yeast RNA helicase, is mutant in ataxia-ocular apraxia 2. Nat Genet 2004;36:225–7.
[19] Puls I, Jonnakuty C, LaMonte BH, Holzbaur EL, Tokito M, Mann E, et al. Mutant dynactin in motor neuron disease. Nat Genet 2003;33:455–6.
[20] Watanabe M, Aoki M, Abe K, Shoji M, Iizuka T, Ikeda Y, et al. A novel missense point mutation (S134N) of the Cu/Zn superoxide dismutase gene in a patient with familial motor neuron disease. Hum Mutat 1997;9:69–71.
[21] Watanabe M, Jackson M, Ikeda M, Mizushima K, Amari M, Takatama M, et al. Genetic analysis of the cystatin C gene in familial and sporadic ALS patients. Brain Res 2006;1073–1074:20–4.
[22] Kadokura A, Yamazaki T, Kakuda S, Makioka K, Lemere CA, Fujita Y, et al. Phosphorylation-dependent TDP-43 antibody detects intraneuronal dot-like structures showing morphological characters of granulovacuolar degeneration. Neurosci Lett 2009;463:87–92.
[23] Stewart HG, Mackenzie IR, Eisen A, Brannstrom T, Marklund SL, Andersen PM. Clinicopathological phenotype of ALS with a novel G72C SOD1 gene mutation mimicking a myopathy. Muscle Nerve 2006;33:701–6.
[24] Ticozzi N, Silani V, LeClerc AL, Keagle P, Gellera C, Ratti A, et al. Analysis of FUS gene mutation in familial amyotrophic lateral sclerosis within an Italian cohort. Neurology 2009;73:1180–5.
[25] Corrado L, Del Bo R, Castellotti B, Ratti A, Cereda C, Penco S, et al. Mutations of FUS gene in sporadic amyotrophic lateral sclerosis. J Med Genet 2010;47:190–4.
[26] Belzil VV, Valdmanis PN, Dion PA, Daoud H, Kabashi E, Noreau A, et al. Mutations in FUS cause FALS and SALS in French and French Canadian populations. Neurology 2009;73:1176–9.
[27] Cudkowicz ME, McKenna-Yasek D, Sapp PE, Chin W, Geller B, Hayden DL, et al. Epidemiology of mutations in superoxide dismutase in amyotrophic lateral sclerosis. Ann Neurol 1997;41:210–21.
[28] Blair IP, Williams KL, Warraich ST, Durnall JC, Thoeng AD, Manavis J, et al. FUS mutations in amyotrophic lateral sclerosis: clinical, pathological, neurophysiological and genetic analysis. J Neurol Neurosurg Psychiatry 2009;81:639–45.
[29] Munoz DG, Neumann M, Kusaka H, Yokota O, Ishihara K, Terada S, et al. FUS pathology in basophilic inclusion body disease. Acta Neuropathol 2009;118:617–27.
[30] Neumann M, Rademakers R, Roeber S, Baker M, Kretzschmar HA, Mackenzie IR. A new subtype of frontotemporal lobar degeneration with FUS pathology. Brain 2009;132:2922–31.

Familial amyloid polyneuropathy (Finnish type) presenting multiple cranial nerve deficits with carpal tunnel syndrome and orthostatic hypotension

Kouki Makioka*, Masaki Ikeda*, Yoshio Ikeda†, Ai Nakasone*, Tenshi Osawa*, Atsushi Sasaki‡, Tomohiro Otani§, Masashi Arai¶ and Koichi Okamoto*

**Department of Neurology*
**‡Department of Human Pathology and*
**§Department of Ophthalmology, Graduate School of Medicine, Gunma University, Maebashi, Gunma, Japan*
**†Department of Neurology, Graduate School of Medicine and Dentistry, Okayama University, Okayama, Japan*
**¶Department of Neurology, Isesaki Municipal Hospital, Isesaki, Gunma, Japan*

Familial amyloid polyneuropathy, Finnish type (FAF), is a dominantly inherited disorder caused by mutations in the gelsolin gene and rarely reported in several countries. We report a Japanese FAF patient with a missense mutation (G654A), presenting multiple cranial nerve symptoms, corneal lattice dystrophy, carpal tunnel syndrome and orthostatic hypotension. It is notable that this patient showed very wide range of cranial nerve involvement (III, IV, VI, VII, VIII, IX, X and XII), which have gradually deteriorated for 6 years. The patient also has carpal tunnel syndrome, which is not commonly found in FAF cases. Even if not for certain familial inheritance, it is preferable to take consideration of FAF as one of differential diagnoses of a case presenting multiple cranial nerves symptoms.

Keywords: Familial amyloid polyneuropathy (FAP type VI), FAP, Finnish type (FAF), gelsolin mutation (G654A), orthostatic hypotension, carpal tunnel syndrome (CTS)

Familial amyloid polyneuropathy is an autosomal dominant disorder caused by mutant gelsolin [FAP, Finnish type (FAF); also known as FAP type IV] initially described by Meretoja in 1969[1]. Familial amyloid polyneuropathy, Finnish type cases have been reported in a limited number of countries such, as Finland, a few other European countries, United States and Japan[2]. Clinical features of FAF include multiple cranial neuropathies, corneal lattice dystrophy and skin changes (cutis laxia and lichen amyloidosus)[1,3,4]. Autonomic nervous disturbance of patients with FAF have been reported in several cases[3–5]. Mild and predominantly sensory affected carpal tunnel syndrome (CTS) has also been described[6]. Missense mutations in the gelsolin gene have been found to be G-to-A or T substitutions at nucleotide 654 (G654A or G654T, respectively), resulting in an amino acid exchange at position 187 (D187N or D187Y)[7,8]. Biochemical studies have indicated that the formation of amyloid fibrils in FAF might be related to mutant gelsolin[9].

A 78-year-old Japanese woman from a family living in Gunma prefecture, a central area of a main

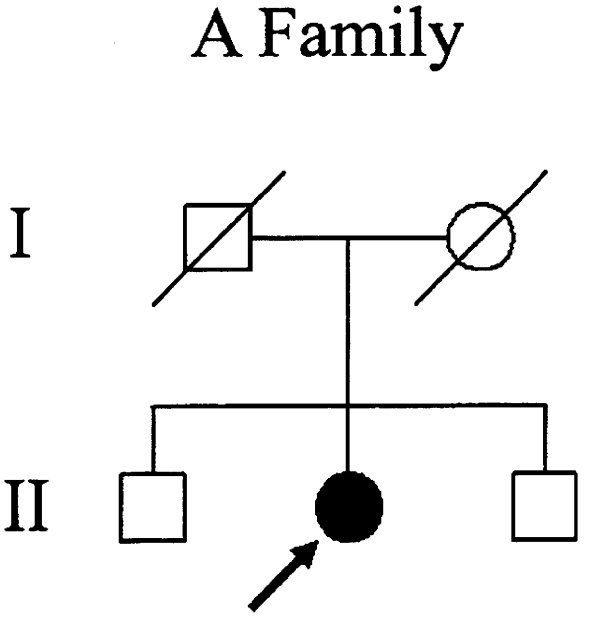

Figure 1 **Pedigree of family A. Male family members are represented by squares, females by circles, deceased members by oblique lines and affected members by solid symbols. The proband is indicated by an arrow (II-2). Both I-1 and I-2 did not present bilateral facial palsies and other cranial nerves signs**

Correspondence and reprint requests to: M. Ikeda, Department of Neurology, Graduate School of Medicine, Gunma University, 3-39-22 Showa-machi, Maebashi, Gunma 371-8511, Japan. [mikeda@med.gunma-u.ac.jp] Accepted for publication January 2009.

© W. S. Maney & Son Ltd 2010
DOI 10.1179/174313209X409007

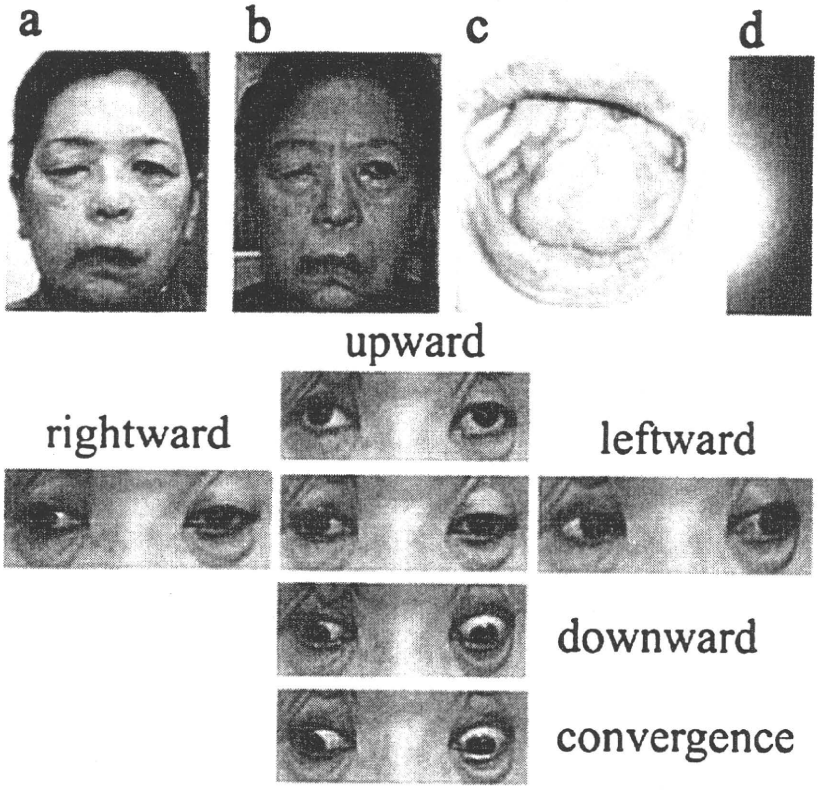

Figure 2 Facial appearance of the proband. (a) Appearance of the proband (II-2) on July 2000. Her face presented bilateral facial palsies in the forehead and skin relaxation (cutis laxa) of the forehead, right upper lids, cheek and angle of the mouth with right dominance. Left perioral angle showed downward hemifacial paresis more than the right. (b) Appearance of the proband (II-2) at July 2006. As ophthalmological operation of upper lid elevation was performed in 2005, the left eye opened clearly; however, the right eye was unable to open because of severe blepharoptosis. Bilateral facial palsies and skin relaxation (cutis laxa) of the forehead, upper lids, cheek and angle of the mouth revealed dominantly on the right. (c) Severe atrophy of the tongue shown especially in the central and peripheral areas in 2000. (d) Slit lamp microscopy examination revealed scattered streaks on the cornea, the findings of corneal lattice dystrophy (type II), which were characteristic of FAF. Lower column: external ocular movement. External ocular movement showed in all directions in the proband (II-2). These findings showed that bilateral abducens nerves suffered paralysis slightly and other directional movement (vertical and internal) caused by oculomotor and trochlear nerves. These findings meant that cranial nerves of III, IV and VI suffered

island in Japan, for many generations and has no relationship with Finnish ancestors and other Japanese FAF families reported previously (II-2, *Figure 1*). At the age of 61 years, when she suffered from left hemifacial spasm and palsy, she was operated with microvascular decompression for left hemifacial spasm. Her facial spasm seemed to be slightly improved; however, the same symptom appeared again. Right blepharoptosis started at the age of 66 years old. She presented dysarthria, swallowing disturbance, hearing loss and tinnitus of bilateral ears at the age of 69 years; thereafter, these symptoms have continued. As she complained deterioration of the facial diplegia, facial spasm and bilateral tongue atrophy at the age of 72 years, she was admitted to our hospital. Her parents died of unrelated disease conditions at their early 50s. There is no family history of the same disorder in her parents and their relatives until their death.

In the physical findings of this patient in 2000, facial appearance looked loose with drooping mouth angles, presenting bilateral peripheral facial palsies and blepharoptosis with right side dominance (*Figure 2a*). At this time, she also showed bilateral fasciculation and tongue atrophy (*Figure 2c*), without skin change as exanthema of lichen amyloidosus. Slit lamp microscopy examination revealed scattered streaks on the cornea, the findings of corneal lattice dystrophy (type II), which were characteristic of FAF (*Figure 2d*). Six year later, an ophthalmological operation for the elevation of left upper eyelid was performed because the left blepharoptosis has severely deteriorated. Bilateral facial paresis deteriorated especially in perioral areas and the left cheek and seemed to be a pendulous skin called 'cutis laxa' (*Figure 2b*). Neurological examination at the time of admission includes multiple cranial neuropathies: III, IV, VI, bilateral blepharoptosis (right dominant) and external ophthalmoplegia for all directions (*Figure 2*, lower column); VII, bilateral facial nerve palsies and fasciculation with right dominance; VIII, bilateral sensorineural hearing disturbance with left dominance; IX and X, poor elevation of soft palate and swallowing difficulty; XII, severe tongue atrophy and prominent fasciculation. In addition to cranial neuropathies, bilateral atrophy of thenar muscles in

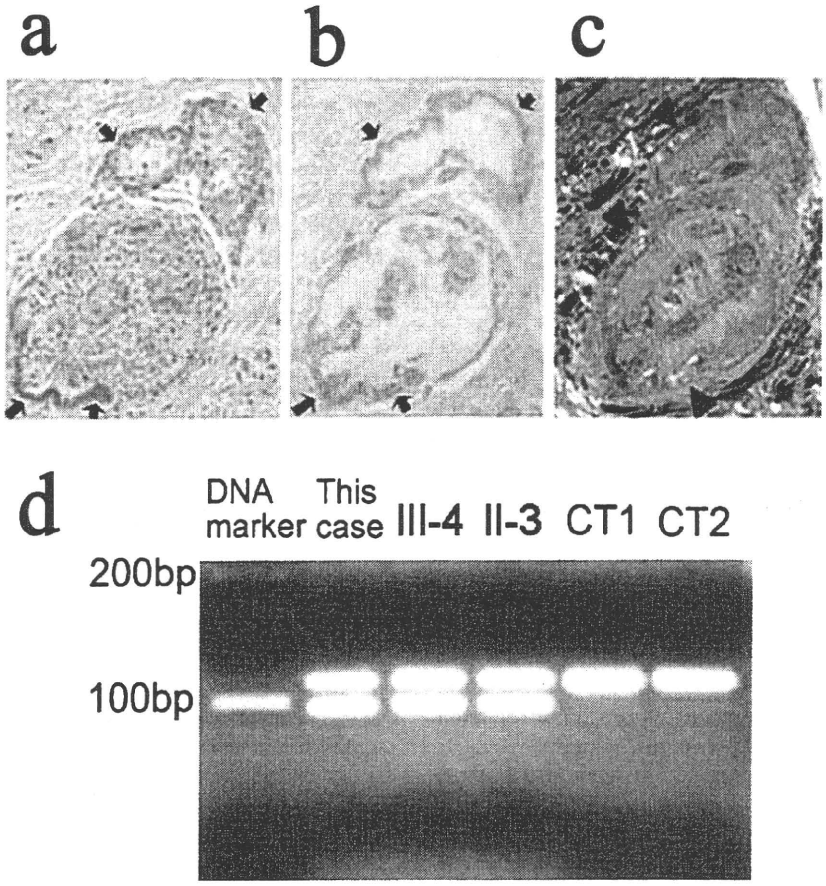

Figure 3 Immunocytochemistry and Congo red stain. (a) Immunocytochemistry of human gelsolin antibody (G4896) revealed immunopositive structure along the sweat glands walls (arrows). (b) Congo red stain showed the same areas as positive-stained areas along the sweat glands walls (arrows). (c) Polarizing microscopy of Congo red stain revealed the same positive structures along the sweat glands walls (arrowhead). (d) Restriction enzyme assay of the polymerase chain reaction (PCR) product using a modified primer in 3·5% agarose gel. Polymerase chain reaction products of this case (II-2) of family A and II-3 and III-4 of family S[11] were digested to 116 and 90 bp by the MfeI enzyme. Polymerase chain reaction products of CT1 and CT2 as control subjects were not digested at the mutation site, so that only 116 bp appeared

her hands was observed. Subjective and objective sensory disturbances were not apparent upon neurological examination. Deep tendon reflexes were normal in all limbs.

The distal latency of compound motor action potential (CMAP) was delayed and low amplitude of bilateral CMAPs was observed in bilateral median nerves, while motor and sensory conduction velocities of bilateral median nerves between elbow and wrist joints were normal. Sensory nerve action potential (SNAP) of the right median nerve could not be detected, and the SNAP and velocity of the left palmar wrist were delayed in the left median nerve (data not shown). These results of neurophysiological studies were compatible with the criteria for bilateral CTS. Head-up tilt examination showed orthostatic hypotension with a decrease in systolic blood pressure from 120 to 90 mmHg.

Skin tissue from left forearm was histologically evaluated. The sample was fixed in 4% paraformaldehyde and embedded in paraffin. The immunocytochemistry using antigelsolin monoclonal antibody (1 : 1000, Sigma) was performed according to previous methods[10,11]. The eccrine sweat glands were outlined by gelsolin-positive immunoreactivity (*Figure 3a*, arrows). Congo red staining showed positive signal at the outline of eccrine sweat glands (*Figure 3b*, arrows), demonstrating yellow-green birefringence of the deposits at the same area in polarizing microscopy, which were compatible with the reported pathological findings of FAF (*Figure 3c*, arrowhead).

After obtaining informed consent for the genetic test, genomic DNA of the proband was extracted from peripheral lymphocytes. A DNA fragment containing codon 187 (116 bp) was amplified by polymerase chain reaction (PCR) using the primers described previously[9]. The primer sequences were as follows: primer A (forward), 5′-TGGTGGTGCAGAGACTCTTCC-3′; primer B (reverse), 5′-GTTGCCCAGGTCCAGGAT-3′. One microgram of genomic DNA was mixed with 0·5 μg of each primer, followed by amplification through 30 cycles under the following conditions: 94°C for 30 seconds for denaturation, 60°C for 30 seconds for annealing and 72°C for 30 seconds for elongation. The PCR product was gel purified and then subjected to direct sequencing using ABI Prism 3100 Genetic analyser DNA sequencer (Applied Biosystems, Foster City, CA, USA). To confirm missense mutation at the codon

187, we used a modified mismatched PCR for restriction analysis as reported elsewhere with the primer A and modified primer B′ (5′-GTTGCC-CAGGTCCAGGATGAAGCAAT-3′)[10,11]. Primer B′ has a mismatched adenine residue at the second position from the 3′ end and generates an MfeI recognition site only if the guanine to adenine substitution occurs at nucleotide 654 of the gelsolin gene. The missense mutation of gelsolin gene was found in the proband as G654A (G-to-A transition at nucleotide 654) at codon 187 resulting in the substitution of aspartic acid to asparagine (not shown). The MfeI (New England Biolaboratory) digestion of PCR product from the proband showed mutant (digested) and wild-type (undigested) fragments heterozygously (*Figure 3d*). The same missense mutation was not detected in 100 normal control alleles.

To date, most of the FAF cases were reported from Finland, especially in the southeastern region[1]. The estimated number of affected Finnish patients is presumably >400 (Ref. 3). Most of them have the G654A mutation resulting in amino acid substitution at D187N, and the same mutation was also reported in Holland[8], the United States[13], Japan[10,11,12–16], Portugal[17] and France[18]. Czech, Danish and French FAF families have carried a G654T mutation resulting in D187Y[8,18]. The present case showed multiple cranial nerve involvement affecting eye movement, which was an infrequently reported symptom characteristic of this case[3,8,10,11,12–18].

In addition to multiple cranial nerve symptoms, this case showed asymptomatic CTS and orthostatic hypotension, while superficial skin change of peculiar exanthema is not prominent as 'lichen amyloidosus' or itching of skin.

An autonomic dysfunction has been reported ~43% in FAF cases (13/30), including orthostatic hypotension, dysfunction of perspiration, gastrointestinal and urinary systems[3]. Autonomic failure of FAF patients showing orthostatic hypotension[12] and dysfunction of perspiration were reported in other FAF cases from Japan[13]. The aberrant electrophysical findings of CTS were found in 18 of 30 FAF patients[6]. In this work, four FAF patients developed symptomatic CTS, and three of them were symptom-free after surgical treatment. Although symptomatic CTS in FAF is not common, subclinical CTS observed in more than half of FAF cases indicates systemic peripheral nerve involvement in FAF[6].

So far, the *de novo* mutation of gelsolin gene has not been reported in FAF patients yet. It is difficult to confirm familial occurrence in this patient because her father and mother died of non-neurological diseases in their 50s and 40s, respectively, before the onset of the proband. Although wide varieties of neurological symptoms in FAF patients were reported, not only facial and lower cranial nerve symptoms but also upper cranial nerve involvement and CTS were characteristics of this case. The reason why missense mutation of gelsolin leads to a variety of clinical symptoms is still unclear. Even if familial occurrence is unclear, it is desirable to take into consideration that FAF can be one of the important differential diagnoses of a patient presenting bilateral multiple cranial nerve symptoms.

Acknowledgement

We thank Professor Yoichi Nakazato and Dr Junko Hirato for their technical supports.

References

1 Meretoja J. Familial systemic paramyloidosis with lattice dystrophy of the cornea, progressive cranial neuropathy, skin changes and various internal symptoms. A previously unrecognized heritable syndrome. *Ann Clin Res* 1969; **1**: 314–324
2 Reilly MM, King RH. Familial amyloid polyneuropathy. *Brain Pathol* 1993; **3**: 165–176
3 Kiuru-Enari S. Familial amyloidosis of the Finnish type (FAF) – a clinical study of 30 patients. *Acta Neurol (Scand)* 1992; **86**: 346–353
4 Kiuru-Enari S. Gelsolin-related familial amyloidosis, Finnish type (FAF), and its variants found world wide. *Amyloid* 1998; **5**: 55–66
5 Kiuru S,"" Matikainen E. Autonomic nervous system and cardiac involvement in familial amyloidosis, Finnish type (FAF). *J Neurol Sci* 1994; **126**: 40–48
6 Kiuru S, Seppalainen AM. Neuropathy in familial amyloidosis, Finnish type (FAF): Electrophysiological studies. *Muscle Nerve* 1994; **17**: 299–304
7 Ghiso J, Haltia M, Prelli F, *et al.* Gelsolin variant (Asn-187) in familial amyloidosis, Finnish type. *Biochem J* 1990; **272**: 827–830
8 de la Chapelle A, Tolvanen R, Boysen G, *et al.* Gelsolin-derived familial amyloidosis caused by asparagine or tyrosine substitution for aspartic acid at residue 187. *Nat Genet* 1992; **2**: 157–160
9 Maury CP, Nurmiaho-Lassila EL, Rossi H. Amyloid fibril formation in gelsolin-derived amyloidosis. *Lab Invest* 1994; **70**: 558–564
10 Sunada Y, Shimizu T, Nakase H, *et al.* Inherited amyloid polyneuropathy type IV (gelsolin variant) in a Japanese family. *Ann Neurol* 1993; **33**: 57–62
11 Ikeda M, Mizushima K, Fujita Y, *et al.* Familial amyloid polyneuropathy (Finnish type) in a Japanese family: Clinical features and immunocytochemical studies. *J Neurol Sci* 2007; **252**: 4–8
12 Gorevic PD, Munoz PC, Gorgone G, *et al.* Amyloidosis due to a mutation of the gelsolin gene in an American family with lattice corneal dystrophy type II. *N Engl J Med* 1991: **325**: 1780–1785
13 Makishita H, Yazaki M, Matsuda M, *et al.* Familial amyloid polyneuropathy type IV (Finnish type) – A clinicopathological study. *Rinsho Shinkeigaku* 1994; **34**: 431–437
14 Ishiguchi H, Shimoya K, Ohnishi A, *et al.* Familial amyloidosis, Finnish type with marked anhidrosis. *Rinsho Shinkeigaku* 1996; **36**: 436–441
15 Akiya S, Nishio Y, Ibi K, *et al.* Lattice corneal dystrophy type II associated with familial amyloid polyneuropathy type IV. *Ophthalmology* 1996; **103**: 1106–1110
16 Sadamoto K, Kinoshita M, Honda M. Familial amyloidosis of the Finnish type (FAP) with extraocular muscle involvement. *Rinsho Shinkeigaku* 1995; **35**: 1034–1036
17 Conceicao I, Sales-Luis ML, Carvalho M-D, *et al.* Gelsolin-related familial amyloidosis, Finnish type, in a Portuguese family: Clinical and neurophysiological studies. *Muscle Nerve* 2003; **28**: 715–721
18 Contegal F, Bidot S, Thauvin C, *et al.* [Finnish amyloid polyneuropathy in a French patient]. *Rev Neurol (Paris)* 2006; **162**: 997–1001

Journal of the Neurological Sciences 297 (2010) 60–65

Contents lists available at ScienceDirect

Journal of the Neurological Sciences

journal homepage: www.elsevier.com/locate/jns

Involvement of endoplasmic reticulum stress defined by activated unfolded protein response in multiple system atrophy

Kouki Makioka [a], Tsuneo Yamazaki [a,*], Yukio Fujita [a], Masamitsu Takatama [b], Yoichi Nakazato [c], Koichi Okamoto [a]

[a] Department of Neurology, Gunma University Graduate School of Medicine, Gunma, Japan
[b] Geriatric Research Institute and Hospital, Gunma, Japan
[c] Department of Human Pathology, Gunma University Graduate School of Medicine, Gunma, Japan

ARTICLE INFO

Article history:
Received 23 April 2010
Received in revised form 16 June 2010
Accepted 17 June 2010
Available online 29 July 2010

Keywords:
Multiple system atrophy
Endoplasmic reticulum stress
Unfolded protein response
α-Synuclein
Granulovacuolar degeneration

ABSTRACT

Multiple system atrophy (MSA) and Parkinson's disease (PD) are classified as synucleinopathies that exhibit α-synuclein deposition in the central nervous system. Recently, activation of the unfolded protein response (UPR), which is a cellular stress response triggered by endoplasmic reticulum (ER) stress, was reported in PD and involvement of ER stress was indicated for this disease. To elucidate whether ER stress is also implicated in the pathology of MSA, we performed a series of immunohistochemical studies using MSA brain sections. Here, we showed the presence of an activated UPR response in oligodendroglia of postmortem MSA brains. The UPR protein-positive structures were observed in lesions where glial cytoplasmic inclusions (GCIs) appeared and colocalized highly in cells showing oligodendrocytic characteristics in the presence of α-synuclein inclusions. The UPR protein-positive structures appeared as granular shapes that are morphologically similar to granulovacuolar degeneration (GVD) and colocalized with GVD marker proteins. Double immunohistochemistry demonstrated that some of the activated UPR protein-positive structures were localized in oligodendrocytes that contained GCIs with faint α-synuclein labeling, without ubiquitination, and showing a strong correlation with the relocation of the tubulin polymerization-promoting protein (TPPP/p25α). These findings suggest that activation of the UPR may be induced at the early stage of the disease process, thus playing a pivotal role in the pathology of MSA.

© 2010 Elsevier B.V. All rights reserved.

1. Introduction

Accumulation and deposition of misfolded proteins is a common sign of neurodegenerative disease, such as Alzheimer disease (AD), Parkinson disease (PD), amyotrophic lateral sclerosis, and polyglutamine diseases [1–4]. The regional distribution in the brain and the composition of protein aggregates are different in each neurodegenerative disease [5]. For example, deposition of amyloid β protein and phosphorylated tau (pTau), and accumulation of α-synuclein in Lewy bodies are the main pathological features of AD and PD, respectively [1,2].

Recently, involvement of endoplasmic reticulum (ER) stress was suggested for AD and PD [6–8]. The ER is an organelle that is important for the synthesis, correct folding, posttranslational modification, and transport of nascent proteins. The presence of a protein overload in the ER that exceeds its folding capacity results in ER stress. In the course of ER stress, signaling pathways that act to protect cells against the toxic buildup of misfolded protein, including the unfolded protein response (UPR), are activated [9–11]. Hoozemans et al. reported that the UPR was activated in dopaminergic neurons in the substantia nigra of PD patients, and that the reaction was observed exclusively in neurons containing α-synuclein [6]. Moreover, overexpression of wild-type or mutant α-synuclein reportedly induces ER stress in cultured cells [12,13]. Thus, these findings suggest the involvement of ER stress in the pathogenic mechanisms of this disease, especially in correlation with α-synuclein accumulation.

Intracellular accumulation of α-synuclein is also a pathological feature of multiple system atrophy (MSA). MSA is a sporadic neurodegenerative disorder that is characterized by neuronal loss accompanied by gliosis in the basal ganglia, cerebellum, pons, inferior olivary nuclei, and spinal cord [14]. The histopathological features of MSA are the presence of argyrophilic glial cytoplasmic inclusions (GCIs) in oligodendroglia [15–17], which contain α-synuclein as their main component [18–21]. Interestingly, UPR is activated in not only neuron but also oligodendroglia in Pelizeus–Merzbacher disease, a neurodegenerative disease causing diffuse hypomyelination of the central nervous system [22]. These findings motivated us to study the involvement of ER stress in the disease mechanisms of MSA. In this study, we used immunohistochemistry to show the presence of an activated UPR reaction in oligodendroglia of MSA samples. The

* Corresponding author. Tel.: +81 27 220 8064; fax: +81 27 220 8068.
E-mail address: tsuneoy@med.gunma-u.ac.jp (T. Yamazaki).

0022-510X/$ – see front matter © 2010 Elsevier B.V. All rights reserved.
doi:10.1016/j.jns.2010.06.019

reaction was observed in cells exhibiting a relatively early phase of α-synuclein deposition and that localized in granular structures that showed morphological characteristics of granulovacuolar degeneration (GVD).

2. Materials and methods

2.1. Antibodies

The commercially available antibodies used in this study were anti-phosphorylated pancreatic ER kinase (pPERK) (phosphorylated PERK at threonine 981) (rabbit polyclonal; Santa Cruz Biotechnology, Santa Cruz, CA) [6,7], anti-phosphorylated eukaryotic initiation factor 2α (eIF2α) (phosphorylated at serine 51, rabbit polyclonal; Cell Signaling, Danvers, MA) [23], anti-phosphorylated inositol requiring enzyme 1α (IRE1α) (phosphorylated at serine 724, rabbit polyclonal; Novus Biologicals, Littleton, CO) [7], anti-tubulin polymerization-promoting protein (TPPP/p25α) (rabbit monoclonal; Epitomics Inc., Burlingame, CA) [24], anti-transferrin (rabbit polyclonal; Dako Cytomation, Glostrup, Denmark) [25,26], anti-Olig2 (rabbit polyclonal; IBL, Takasaki, Japan) [27], anti-glial fibrillary acidic protein (GFAP) (rabbit polyclonal;Dako Cytomation, Glostrup, Denmark) [28], anti-α-synuclein (mouse monoclonal; Invitrogen, Carlsbad, CA) [29], anti-ubiquitin (rabbit polyclonal; Dako Cytomation, Glostrup, Denmark) [30,31], anti-tau phosphorylated (AT8) (mouse monoclonal; Innogenetics, Ghent, Belgium) [32,33], anti-phosphorylated glycogen synthase kinase (pGSK3) (mouse monoclonal; Upstate Biotechnology, Lake Placid, NY) [33,34], anti-pSmad2/3 (phosphorylated at serine 423 and 425) (goat polyclonal; Santa Cruz Biotechnology, Santa Cruz, CA) [33,35], and anti-phosphorylated neurofilament (SMI-31) (mouse monoclonal; Sternberger Monoclonals, Baltimore, MD) [33,36]. The generation and characterization of the antibody that recognizes phosphorylated TAR-DNA-binding protein 43 (pTDP-43) at positions 409 and 410 (A2) was described elsewhere [33].

2.2. Immunohistochemistry

Brain tissues were obtained from 12 subjects (average age, 59.8 years; six males and six females) who had a neuropathologically confirmed diagnosis of MSA, and from five control subjects (average age, 60.2 years; two males and three females) who died of cancer, stroke, pneumonia, or myocardial infarction (Table 1) with no signs of neurodegeneration. In addition to the MSA cases, two samples of a hereditary type of spinocerebellar degeneration (SCD), which were diagnosed as Menzel-type SCD at death, were also examined. These cases were autopsied before the findings of causative genes; thus, gene analysis was not carried out. However, the neuropathological findings of these cases were typical of olivopontocerebellar atrophy (OPCA), and GCIs were absent [15].

Five-micrometer-thick sections of formalin-fixed, paraffin-embedded tissues from the cerebellum, pons, and striatum were immunostained with the appropriate antibodies using the streptavidin–biotin method (Histofine SAB-PO kit; Nichirei, Tokyo, Japan). For all stainings, sections were deparaffinized and subsequently immersed in 0.3% hydrogen peroxide (H_2O_2) (Dojin Laboratories, Kumamoto, Japan) in methanol for 30 min to block endogenous peroxidase activity. For the detection of peIF2α, pIRE1α, TPPP/p25α, and pTDP-43, sections were autoclaved for 10 min in 10 mM sodium citrate buffer (pH 6.0), for antigen retrieval. Immunoreactivity was visualized using 0.5 mg/ml 3,3′-diaminobenzidine tetrachloride (DAB) and 0.03% H_2O_2 (Dojin Laboratories, Kumamoto, Japan). To assess the detailed colocalization of proteins in cells, double immunohistochemistry was performed in a subset of sections [7]. After incubation with the second primary antibody, specimens were treated with the avidin–biotin/alkaline phosphatase complex (VECTASTAIN® ABC-AP KIT; Vector Laboratories, Burlingame, CA) and the colorimetric reaction was developed using the Vector® Red Alkaline Phosphatase Substrate Kit as a chromogen. All sections were counterstained with hematoxylin. The specimens were observed under an Olympus BX60 microscope (Olympus, Tokyo, Japan) using the DP Controller software.

For the evaluation of the relationship between pPERK-positive structures and α-synuclein, ubiquitin, and TPPP/p25α, we counted 150 cells exhibiting pPERK-positive structures and calculated the protein colocalization ratio.

2.3. Electron microscopy

Twelve-micrometer-thick sections of formalin-fixed, paraffin-embedded tissue from the pons of an MSA case were immunostained with anti-pPERK antibodies using the streptavidin–biotin method. The sections were incubated with 0.5 mg/ml DAB for 30 min and 0.5 mg/ml DAB with 0.03% H_2O_2 for 30 min. After incubation with 2% osmium tetroxide (Chiyoda Junyaku, Tokyo, Japan), the sections were embedded in epoxy resin. The specimens were trimmed and cut into ultra-thin sections. These sections were examined under a JEOL 100CX electron microscope (JEOL, Tokyo, Japan).

2.4. Double immunohistochemistry using fluorescent antibodies

To assess the colocalization of pPERK with pTau, pGSK3, and pSmad2/3, we performed double immunohistochemistry using fluorescent secondary antibodies [33]. After deparaffinization and autoclaving, sections were incubated with the anti-pPERK antibody and each of the other three primary antibodies overnight at 4 °C. The combinations of the secondary antibodies were Alexa Fluor 488 goat anti-rabbit IgG (H + L) (Molecular Probes-Invitrogen, Eugene, OR) and Alexa Fluor 568 goat anti-mouse IgG (H + L) (Molecular Probes-Invitrogen) or Alexa Fluor 488 donkey anti-rabbit IgG (H + L) (Molecular Probes-Invitrogen) and Alexa Fluor 568 donkey anti-goat IgG (H + L) (Molecular Probes-Invitrogen). To avoid autofluorescence signals, sections were treated with Sudan Black B for 5 min and rinsed in 70% ethanol. Specimens were mounted with Vectashield (Vector Laboratories) and examined under a microscope equipped with confocal systems (FV1000; Olympus). The images obtained were processed further using Adobe Photoshop CS2 version 9 (Adobe, San Jose, CA).

Table 1

	Age sex	Middle cerebellar peduncle	White matter of cerebellum	Pontecerebellar fibers	Striatum	GCI
MSA1	66M	++	+++	++	−	+
MSA2	54F	+++	+++	+++	+	+
MSA3	60M	+	+	+	+	+
MSA4	62F	−	−	++	−	+
MSA5	65M	−	++	++	+	+
MSA6	57F	+++	+++	+++	−	+
MSA7	51F	+++	+	++	+	+
MSA8	58F	+++	+++	++	+++	+
MSA9	64M		+	++	−	+
MSA10	64M	+++	+	++	−	+
MSA11	56M	++	+	+	−	+
MSA12	60F		+++	++	++	+
H-SCD1	59F	−	−	−	−	−
H-SCD2	49F	−	−	−	−	−

− 0.3, + 4–10, ++ 10–20, and +++ >20.
Mean counts of pPERK-positive structures per a high power magnification (×400).

3. Results

We first examined the activity of UPR markers (pPERK, peIF2α, and pIRE1α) in brains of normal controls and of patients with neuropathologically proven MSA. Although no immunoreactivity was

detected in control brains, pPERK-positive granular structures were observed near nuclei in some glial cells of all MSA cases (Fig. 1a and b). The pPERK-positive structures were observed in the middle cerebellar peduncle, white matter of the cerebellum, pontocerebellar fibers, and striatum, where GCIs are frequently observed in MSA brains [15,16] (Table 1). These immunopositive structures were not found in the regions that were less affected in MSA. The anti-peIF2α and anti-pIRE1α antibodies also detected the granular structures in MSA brains (Fig. 1c and d). Many of these immunolabeled structures were composed of cores and surrounding vacuoles (Fig. 1b). Central cores showed intense immunoreactivity, whereas outer membranes were stained to a lesser degree (Fig. 1b–d). To investigate these structures in detail, we examined them using immunoelectron microscopy. The immunolabeled structure was composed of a central electron-dense core and a surrounding outer layer (Fig. 1e). Importantly, although the number of samples was small, no immunoreactivity was observed in any of the hereditary-type SCD specimens, which exhibited neurodegeneration in the pons and cerebellum, without GCIs (Fig. 1f). The three antibodies detected the same granular structures in MSA brains; however, the anti-pPERK antibody yielded the most intense immunolabeling, even in the absence of the antigen retrieval treatment. Thus, we decided to use the anti-pPERK antibody primarily for the detection of activated UPR in this study.

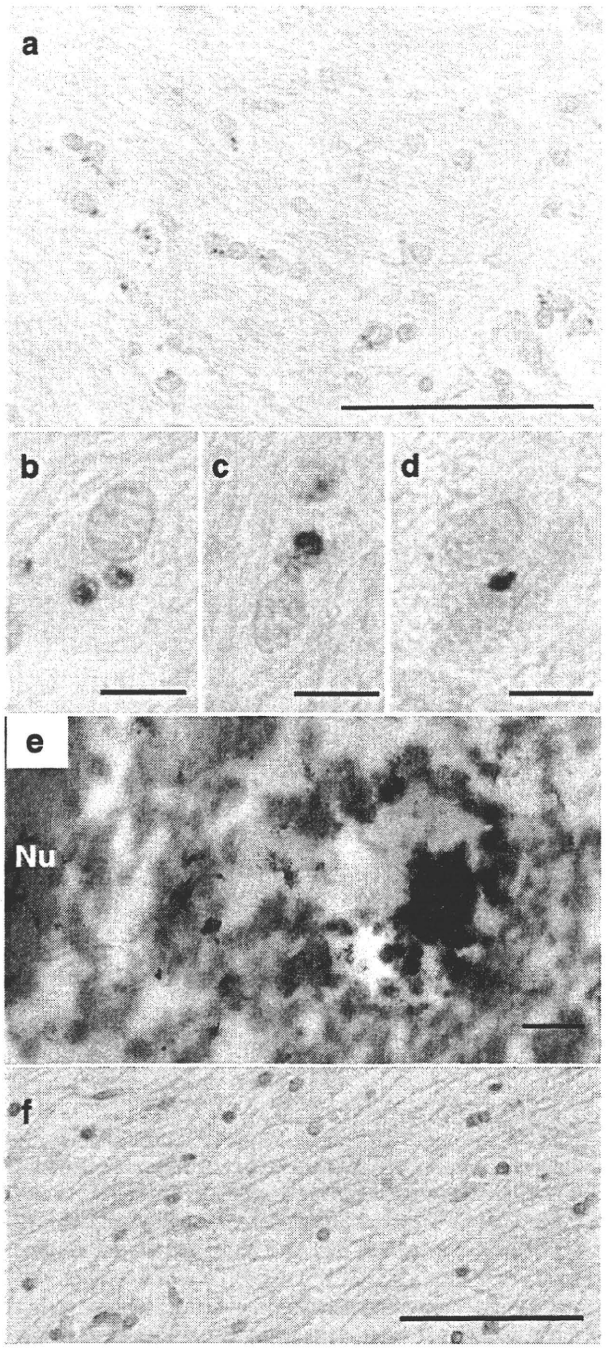

Fig. 1. Immunohistochemical detection of pPERK (a and b), peIF2α (c), pIRE1α (d) in MSA and hereditary SCD (f) brains using microscopy. Immunohistochemical detection of pPERK using electron microscopy (e). The pPERK-positive structures were detected as granules in some glial cells (a and b) and most of them were composed of cores and surrounding sounding outer layer, being compatible with GVD (b and e). Other activated UPR markers, peIF2α (c) and pIRE1α (d), were also detected in granular structures. However, no immunolabeling was observed in hereditary SCD cases lacking GCIs (f, pPERK staining). Scale bars, 100 μm (a and f), 10 μm (b–d), and 1 μm (e). Nu; nucleus.

Because activated UPR proteins localize in GVD in AD [7] and because the morphological characteristics of pPERK-positive granular structures in MSA were similar to those of GVD (Fig. 1b), we examined the colocalization of pPERK with other proteins that are known to be localized in GVD (i.e., pTau, pGSK3, pSmad2/3, and SMI-31) in MSA sections using confocal microscopy. As shown in Fig. 2, pPERK partly colocalized with pTau, pGSK3, and pSmad2/3, but not with SMI-31. These immunoreactions were not observed in sections stained by the same method without primary antibodies, avoiding the possibility that the reactions were due to the autofluorescence (data not shown).

Recently, we demonstrated the localization of pTDP-43 in GVD in AD [33]; thus, we were interested in determining whether pTDP-43 immunoreactivity was observed in MSA. As shown in Fig. 3a, immunoreactivity for pTDP-43 was detected in granular structures in MSA brains where pPERK-positive structures were also present. Double immunohistochemistry showed that a subpopulation of granular structures was labeled with both the anti-pTDP-43 and anti-pPERK antibodies (Fig. 3b); however, some granular structures were independently immuno positive exclusively for pPERK (Fig. 3c) or for pTDP-43 (Fig. 3d).

Because the distribution of cells with pPERK-positive granules was similar to that of GCIs in MSA, and because MSA is considered as a primary oligodendrogliopathy [37], we hypothesized that the immunolabeled structures may be localized in oligodendroglia. To examine this, sections were double labeled with the anti-pPERK antibody and antibodies against oligodendroglial marker proteins. As shown in Fig. 3e–g, pPERK-positive structures were observed in cells that exhibited a transferrin-positive cytoplasm (Fig. 3e) [38] and Olig2-positive nuclei (Fig. 3f) [27]; however, these structures were not detected in GFAP-positive astroglia in the examined sections (Fig. 3g). Immunoreactivity for transferrin and Olig2 is specific to oligodendroglia; thus, we concluded that pPERK-positive granules were present mainly in oligodendrocytes.

To investigate the association of pPERK with α-synuclein, which is a main component of GCIs [18–21], we performed double immunohistochemistry (Fig. 4a). The majority of cells that contained pPERK-positive structures were also positive for α-synuclein (74.3%). Interestingly, the immunoreactivity for α-synuclein in some of those cells tended to be faint (Fig. 4a). As it is known that α-synuclein-positive GCIs become ubiquitinated during the maturation process [39], we examined the association of pPERK and ubiquitinated GCIs. We found that 54.2% of pPERK-positive cells exhibited ubiquitin-positive inclusions (Fig. 4b). These findings suggest that the emergence of pPERK-positive granules may be associated with the formation of GCIs at a relatively early phase.

To examine this issue further, we performed double immunohistochemistry using the anti-pPERK and anti-TPPP/p25α antibodies. TPPP/p25α is expressed predominantly in oligodendroglia, is present in myelin basic protein immunopositive sheaths, and localizes around the nucleus in a thin sheet of cytoplasm [24]. TPPP/p25α promotes the aggregation of α-synuclein [9] and accumulates in the cytoplasm of

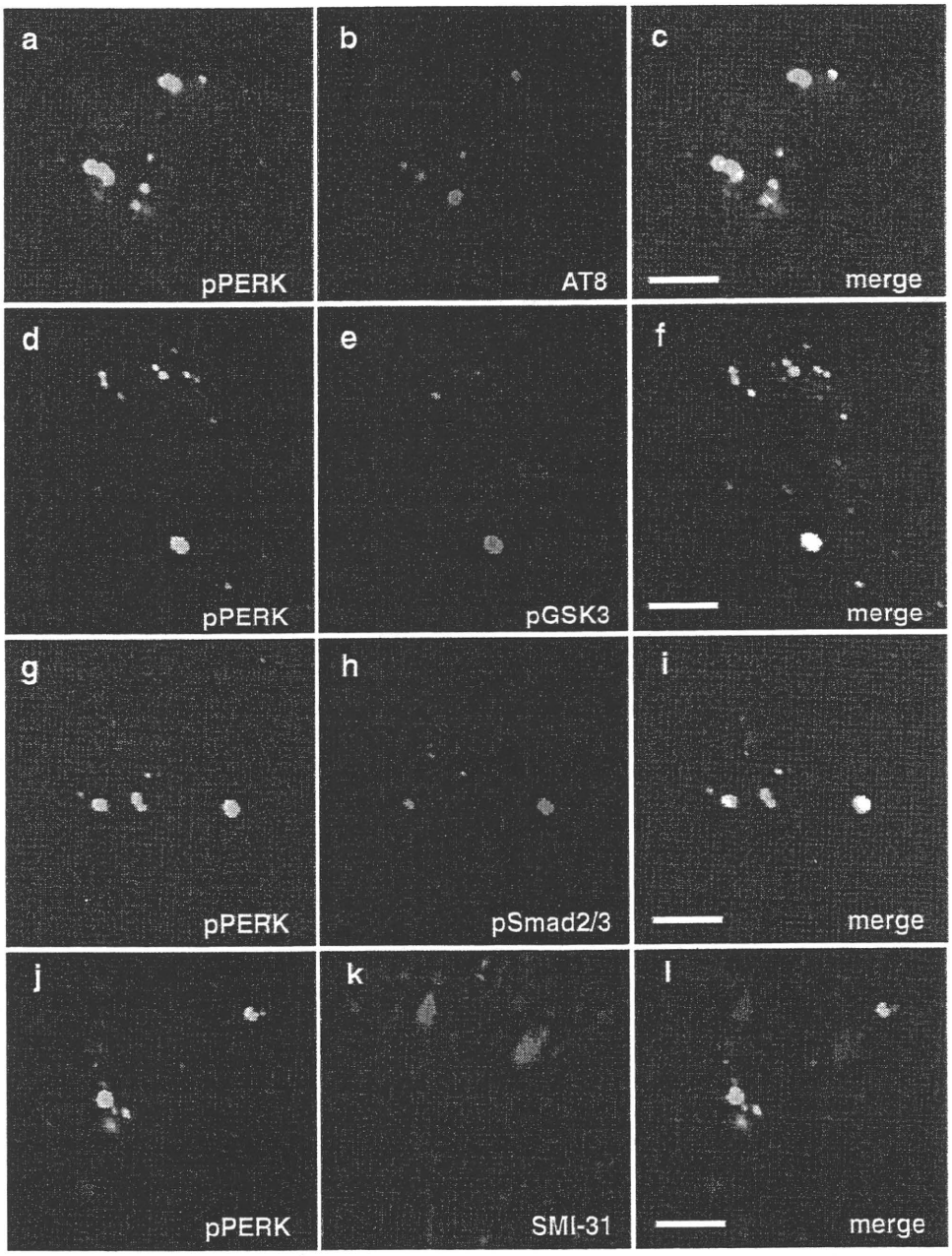

Fig. 2. Double immunohistochemistry for pPERK (green) and GVD markers (pTau, AT8, pGSK3, pSmad2/3, and SMI-31) (red). As shown in merged images, pPERK-positive structures were partly colocalized with pTau (c), pGSK3 (f), and pSmad2/3 (i), but not with SMI-31 (l). Scale bars, 10 μm.

oligodendroglia, away from the myelin sheath, in the early stage of MSA pathology [24,37]. As shown previously, TPPP/p25α relocated from the sheath to the cell bodies in the white matter of the cerebellum of MSA samples (Fig. 4c). Interestingly, granular immunoreactivity of TPPP/p25α, just like a GVD, was also detected (Fig. 4c, inset). Double immunohistochemistry showed that most pPERK-positive structures were located in TPPP/p25α-immunoreactive oligodendrocytic cell bodies (78.7%) (Fig. 4d).

4. Discussion

In this study, we demonstrated for the first time that the UPR, which is a cellular stress response that is triggered by ER stress, was activated in sporadic MSA brains. The activated UPR protein-positive structures emerged in oligodendroglia in lesions containing GCIs [15,16]. Double immunohistochemistry experiments showed that the activated UPR protein-positive structures were localized in cells that also showed immunoreactivity for α-synuclein. Moreover, these immunoreactivities were absent in hereditary SCD cases lacking GCIs. Thus, we concluded that the emergence of activated UPR protein-positive structures may be deeply associated with the disease mechanisms involved in sporadic MSA.

Our double immunohistochemistry results showed that the activated UPR protein-positive structures were localized in cells that showed relatively faint immunoreactivity for α-synuclein (Fig. 4a), and that the ratio of colocalization of the activated UPR protein-positive structures with α-synuclein deposition was greater than that observed for ubiquitin. Wenning et al. demonstrated that the immunoreactivity of α-synuclein is relatively faint during its initial stage of deposition; in addition, ubiquitination of α-synuclein-positive GCIs increases as the disease progresses [40]. Thus, our findings suggest that the activated UPR protein-positive structures

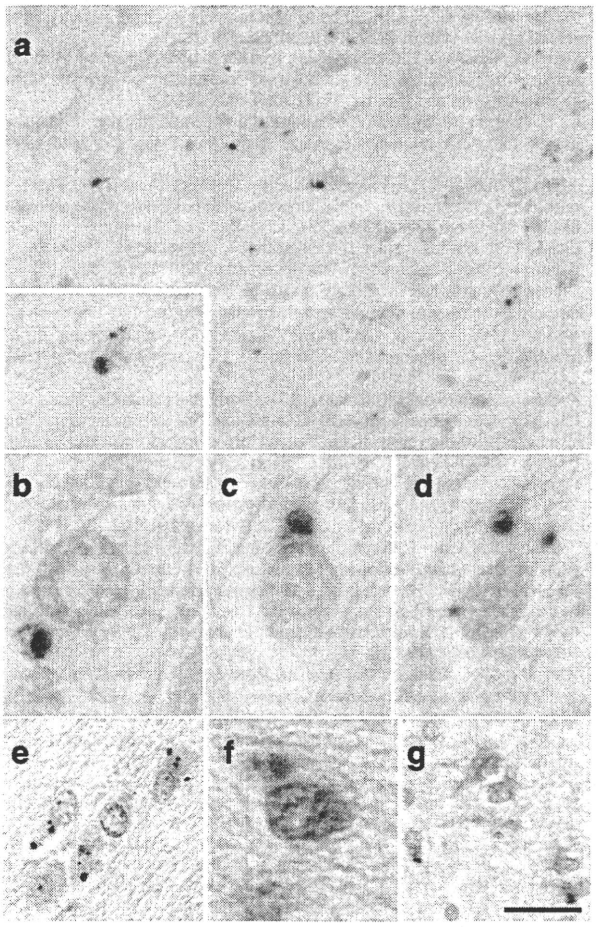

Fig. 3. The phosphorylation-dependent anti-TDP-43 antibody detected granular structures that were observed exclusively in pPERK-stained samples (a, an enlarged image is shown in the inset). Double immunohistochemistry for pTDP-43 (brown) and pPERK (red) demonstrated the frequent colocalization of both proteins in the same structure (b); however, some granules were independently immunolabeled with pPERK exclusively (c) and pTDP-43 (d). The pPERK-positive structures (brown in e and g, red in f) were localized in cells exhibiting positivity for transferrin in the cytoplasm (e) and for Olig2 in the nucleus (f), but not for cytoplasmic GFAP. Scale bars, 100 μm (a), 10 μm (b–d and f), and 20 μm (e and g).

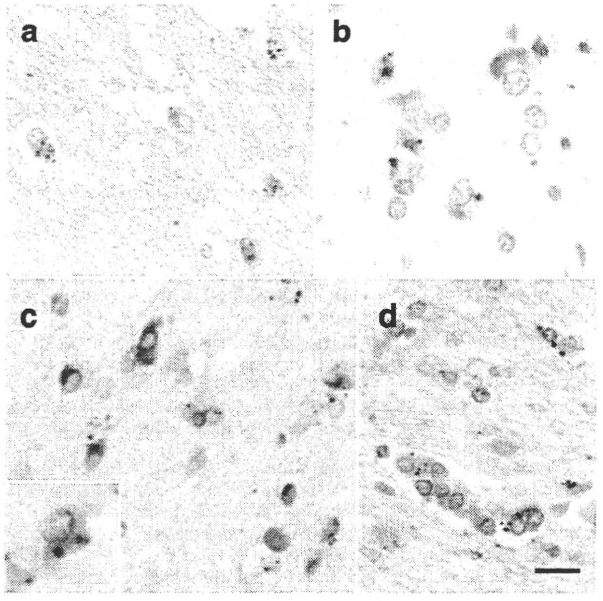

Fig. 4. The pPERK-positive structures (brown in a) were localized in cells exhibiting α-synuclein labeling (red in a) that was frequently faintly positive (a). The pPERK-positive granules (brown in b) were also observed in cells containing ubiquitin-labeled structures (red in b). The TPPP/p25α immunoreactivity was localized diffusely in cell bodies (c) and was also detected in granular structures (c, inset) in MSA cases. Most of the pPERK-positive granules (brown in d) were observed in TPPP/p25α-labeled cells (red in d). Scale bars, 20 μm (b) and 10 μm (a, c, and d).

emerge in the early stages of oligodendroglial pathology in MSA. This notion was also supported by our findings that the emergence of activated UPR protein-positive structures exhibited a strong correlation with the relocation of TPPP/p25α to oligodendrocytes, which occurs in the early stages of the MSA pathology [24,37]. Recently, it was demonstrated that the UPR is activated in pyramidal neurons of the hippocampus of AD patients and in dopaminergic neurons of the substantia nigra of PD brains [6,7,23]. Using immunohistochemistry, these authors showed that immunoreactivity is found in granular structures or in GVD [7,23]. Interestingly, activation of the UPR is observed in pre-tangle neurons in AD [7] and in neurons at the pre-stage of Lewy body formation [6]. These findings, together with our results, suggest that the activated UPR protein-positive structures emerge at the early stage of the disease process in relation to the deposition of key pathological proteins in AD, PD, and MSA. The UPR is activated to reduce the unfolded and misfolded protein load in the ER, and to protect cells against ER stress, which leads to programmed cell death [41]. Thus, it might be reasonable to predict that the appearance of activated UPR-positive structures indicates the involvement of ER stress, and reflects the protection mechanisms that act at early stages of these diseases.

As shown in the figures, activated UPR proteins were located in granular structures, some of which exhibited a morphology that matched that of GVD. Although tubular structures were not detected during the electron microscopy study, because of poor fixation, these structures exhibited features that had some similarity with GVD. GVD is characterized by the presence of basophilic granules, surrounded by a clear zone, that measure 3 to 5 μm in diameter and occur predominantly in hippocampal neurons in AD and aged brains [30,42–45]. GVD in AD brains is immunoreactive for pTau [32], pGSK3 [34], pSmad2/3 [35], SMI-31 [36], and ubiquitin [30,31]. Here, we demonstrated that a fraction of pPERK-positive structures in oligodendroglia of MSA brains were colocalized with pTau, pGSK3, pSmad2/3, and pTDP-43, but not with SMI-31. SMI-31 specifically recognizes phosphorylated neurofilaments with a size of 200 and 160 kDa, which exist exclusively in neuronal cells [46]. Thus, it is reasonable to speculate that the GVD-like pPERK-positive structures detected in non-neuronal cells were immuno-negative for the SMI-31 antibody. This notion is supported by our findings that the pPERK-positive granular structures detected in MSA samples were observed in oligodendroglia-positive cells. To our knowledge, there are no reports demonstrating the emergence of GVD-like structures in oligodendroglia. However, because of the absence of pPERK-positive granules in normal control and hereditary SCD, the formation of the GVD-like structures in oligodendroglia may be disease-specific and may play a pivotal role in MSA pathology. Previously, we demonstrated that the ultrastructural characteristics of GVDs are compatible with autophagosomes [30]; in addition, recent studies suggest that autophagy plays a crucial role in the pathology of AD and PD [47–49]. Moreover, autophagy is induced by ER stress in cultured cells [50,51]. Thus, it might be reasonable to assume that autophagy induced by ER stress may also play a role in the disease mechanisms underlying MSA.

Acknowledgments

This study was supported by grants from the Ministry of Health, Labor and Welfare and from the Ministry of Education, Culture, Sports, Science and Technology of Japan to K. Okamoto.